



# Western Engineering

**MSE 4499 — Mechatronic Design Project**

---

## **LunaTron Terramechanics Terrain Sensor**

by

Nicole Devos

Ushwyn Leach

Jason Tang-Yuk

### **Final Report**

Faculty Advisor: Ken McIsaac

Date Submitted: April 8, 2015

## Executive Summary

This report covers the design of the micro-bevameter LT3S. The idea for this project came directly from Western University PhD candidate, Matthew Cross. Recently, there has been speculation as to whether or not there is water on Earth's moon. In order to both effectively and efficiently map previously unexplored areas, a number of scout rovers could be used to actively seek out items of interest. Once an item of interest is located, the scout rovers could communicate with the master rover and make it aware of the location of the potential discovery. To increase efficiency, a method to estimate the power required to travel a specific path on the lunar surface could be added to these small scout rovers. LunaTron is a terrestrial version of one of these scout rovers. It was first designed last year with the purpose of validating a spaceflight ready version of itself, as well as to test these path planning methods. The LT3S has been designed to validate the experimental terrain data calculated by the LunaTron used in the path planning.

The design of the micro-bevameter was split into four smaller subsystems: the pressure-sinkage device, shear-slippage device, structural design, and controller design. Original concepts and their analysis are discussed briefly. The final design was selected to be a rigid prismatic frame with a top surface to which most components will be mounted. The pressure-sinkage and shear-slippage subsystems were designed similar to a drill press, with a linear actuator, gear motor, and a pulley system to produce the motions required in the device. The design allows for interchangeable base plates, and there are currently three plates manufactured and ready for testing. The selected sensors will measure the torque above the base plate, the force applied to the base plate, and the vertical displacement of the base plate. A single microcontroller was selected to control all components of the device as well as record data from the tests.

The next steps in this project will be to attach the sensors for torque and force on the base plate, and procure and attach a linear bearing to remove the horizontal drift of the shaft. Also, the custom PCB designed for this micro-bevameter needs to be fabricated and tested, a 12V battery and a microSD card purchased, and an optical base plate encoder needs to be designed to increase accuracy and precision in the LT3S's measurements. Once these modifications are made, testing of the accuracy of the LT3S can be done according to the outline included in the report.

The cost of this design was approximately \$500, not including the donated cost of the microcontroller. It is expected the cost of the design will increase with the addition of the circuit board and components, battery, linear bearing, microSD and the design and implementation of the optical base plate encoder. These changes will cost approximately \$200 plus the cost of the encoder design.

Before the LunaTron can produce data to validate, a few improvements must be made. The various onboard sensors need to be calibrated, and three purchased components need to be replaced. These parts need to be machined and calibrated. Ultimately, the final testing of the

path planning is dependent on the progress made in the other LunaTron-based capstone projects.

## Table of Contents

Executive Summary.....	ii
Table of Contents.....	iv
List of Figures.....	vii
List of Tables .....	ix
Introduction.....	1
Design Problem.....	1
Scope.....	1
Background Information .....	2
Design Requirements and Constraints .....	4
State-of-the-Art and Emerging Technologies .....	5
Generation and Evaluation of Concepts .....	6
Pressure-Sinkage Design .....	6
Shear-Slippage Design .....	7
Structural Design .....	7
Microcontroller and UI Design.....	8
Engineering Analysis .....	9
Background Mathematics .....	9
Pressure-Sinkage Mathematical Model .....	9
Shear-Slippage Mathematical Model.....	11
Base Plate Analysis.....	12
Base Plate Design.....	14
Refinement of Design.....	16

Design One.....	16
Design One Refinement.....	17
FEA of Design One.....	19
Design Two.....	21
FEA of Design Two.....	23
Final Design.....	25
Sensor and Actuator Selection.....	27
Mechanical Components.....	28
FEA of Final Design.....	29
Control System.....	31
Prototype Development .....	34
Prototype Construction.....	34
Budget .....	39
Testing and Evaluation .....	41
Modifications and Improvements .....	42
Project Planning and Scheduling .....	43
Conclusion.....	45
Recommendations.....	45
References.....	46
Appendix I – Strain Gauge Formation as a Wheatstone Bridge .....	47
Appendix II – Initial Gantt Chart.....	48
Appendix III - Shaft Selection Analysis .....	49
Appendix IV - Frame Material Analysis.....	53
Appendix V – PCB Components.....	54

Appendix VI – Base Plate Size Script .....	55
Appendix VII – MATLAB Parameter Calculation Script.....	56
Main Script.....	56
Pressure Conversion Function.....	57
Average Pressure Calculation Function.....	58
Interpolation Function .....	58
Pressure-Sinkage Parameter Calculation Function.....	58
N <sub>avg</sub> Calculation Function.....	59
Summations Function.....	59
Shear Conversion Function.....	60
CalculateKExp Function (Exponential output curve) .....	60
CalculateKPeakDown Function (Output curve that peaks then drops).....	61
Appendix VIII – Run Code .....	62
Appendix IX – Part and Assembly Drawings .....	70

---

## List of Figures

Figure 1: The Kapvik rover.....	2
Figure 2: A Vane Cone Device. ....	5
Figure 3: Three structural designs, the cubic casing (a), the cylindrical casing (b) and the tripod design (c). .....	8
Figure 4: Diagram of rigid wheel in contact with terrain. W is the weight on the wheels; T is the torque driving the wheels; w is the rotational velocity of the wheel; $\theta_c$ is the wheel-terrain contact angle. [2].....	13
Figure 5: Final base plate design mounted on shaft. ....	15
Figure 6: SolidWorks model of initial design.....	17
Figure 7: SolidWorks model of design one following the first round of iterations. ....	18
Figure 8: FEA static nodal stress plot of design one. ....	20
Figure 9: FEA static nodal displacement plot of design one, focused on the guide rails. ....	20
Figure 10: Linear Mechanism on Shaft (Top down: Shaft Collar, Ball Bearing, Mounted Ball Bearing, Ball Bearing, and Shaft Collar).....	22
Figure 11: Reduced size of structural frame. ....	23
Figure 12: FEA of final design, Von Mises (left) and Displacement (right).....	25
Figure 13: Final prototype design. 1. Base plate. 2. Linear actuator design. 3. Gearmotor assembly.....	26
Figure 14: FEA pressure sinkage .....	30
Figure 15: Shear slippage test.....	30
16: Control system flow chart.....	32
Figure 18: PCB design for an Intel Galileo shield.....	33
Figure 19: Prototype with all components. ....	35
Figure 20: Linear actuator coupled with main shaft.....	36

Figure 21: Gearmotor coupled to shaft.....	37
Figure 22: Base plate assembly. ....	38
Figure 23: Strain gauge layout on shaft [6].....	47
Figure 24: Strain gauge circuit layout [6]. .....	47
Figure 25: CES of Shear Modulus and Young's Modulus of potential shaft materials .....	52
Figure 26: CES of Young's Modulus and Cost of potential structural framing materials. ....	53

## List of Tables

Table 1: Functional requirements as provided by project supervisor. ....	4
Table 2: Bekker's parameters for LETE Sand, Sandy and Clayey Loam as reported by Wong [4].....	13
Table 3: Base plate radii for desired wheel sizes calculated for various soil types (See Appendix VI for calculations). .....	14
Table 4: Cost breakdown of mechanical and electrical components.....	39
Table 5: Table of tasks and deliverables, including the original estimated hours and dates, and the final actual hours and dates spent on the tasks. ....	44
Table 6: Available shaft materials and the respective costs for 3 ft. with a 3/4" diameter.....	49
Table 7: Components required for the PCB .....	54

## **Introduction**

### **Design Problem**

The purpose of this design project is to test and verify a method of estimating planetary terrain parameters using a simplified rocker bogie model that was developed by David Michel [1]. To accomplish this, the LunaTron rover needs to be adjusted and re-coded to test Michel's model. Additionally, a sensor will be designed and constructed from the ground up to get accurate, comparable results for the existing LunaTron Rover at Western University. This sensor will provide terramechanical data which will be used to validate wheel design for micro-class rovers.

### **Scope**

The main goal of this project is to validate the terramechanics data being calculated on board the micro-rover, LunaTron. To accomplish this, a micro-bevameter needs to be designed for use with micro-class ( $< 50$  kg) vehicles. The bevameter designed needs to be untethered and portable, in order to test in-situ, as well as be able to perform the pressure-sinkage test and the shear-slippage test for wheels of varying sizes. This project covers the design and implementation as far as the structural, actuator, and basic controller design. The last component needed is an optical encoder for the base plate, although this design is outside the scope of this project.

## **Background Information**

Spirit, a Mars Exploration Rover, ended its mission on Mars after running into an unforeseen obstacle: loose soil. The rover was immobilized in this non-geometric obstacle, and is no longer online. Other exploration rovers have run into this issue, but have been more successful in navigating out – for example, NASA’s Opportunity got trapped in the Purgatory Dune in 2005, and took 5 weeks to successfully extract itself.

Matthew Cross, a graduate student at Western University, is currently researching a low-cost solution to this problem that doesn’t require cumbersome sensory equipment. This method uses a micro-rover named Kapvik with an artificial neural network to estimate two parameters, the soil cohesion,  $c$ , and the shearing resistance angle,  $\Phi$ . Soil with a low cohesion is loose, like gravel or sand, and can cause the rover to slip, lose traction, or get stuck; therefore knowing these parameters can be very useful [2].



Figure 1: The Kapvik rover

To validate this method, we have been asked to create a micro-bevameter to be used in situ to measure wheel-terrain interaction parameters. These include ‘Bekker parameters’ (pressure-sinkage) and ‘Wong parameters’ (shear-slippage) [2,3]. To obtain the pressure-sinkage parameters, a flat plate is pressed to a specified force in a terrain and the depth of penetration of that flat plate is recorded. The shear measurements involve a shear ring base plate being pressed into the soil. The torque required to shear this soil at different depths to varying degrees is then recorded [4]. With these measurements, the cohesion, friction angle and shear deformation parameters of various terrains can be calculated and compared to the values estimated by Cross’s model.

## Design Requirements and Constraints

The final list of requirements for the micro-bevameter, as given by our project supervisor, are listed in Table 1 below.

Table 1: Functional requirements as provided by project supervisor.

Requirement Level		
Requirement Description	Mandatory	Targeted/Desirable
The bevameter shall provide wheel-terrain interaction measurements for wheels of the following diameters:	10 cm	10, 15 and 20 cm
The bevameter shall provide wheel-terrain interaction measurements for wheels of the following widths:	5 cm	5, 7.5 and 10 cm
The bevameter shall provide wheel-terrain interaction measurements for single-wheel loads of up to:	20 N	80 N
The bevameter shall provide as outputs:	Raw data for post processing	The shear strength parameters* and pressure-sinkage relationship parameters
The bevameter must be portable.	Mandatory	N/A
The bevameter shall facilitate data storage.	Mandatory	N/A
The bevameter shall store data in formats compatible with both Microsoft Windows and Unix-based PC's.	Mandatory	N/A

\* c (cohesion, in Pa),  $\phi$  (friction angle, in degrees) and K(shear deformation parameter, in cm)

Along with these, this project had a monetary constraint of \$300, and a weight range: the overall structure must be between 10kg and 20kg; this is to ensure the device is heavy enough to resist the reaction forces of the tests, yet still be portable. A final self-imposed objective to

minimize the complexity of the design was incorporated to ensure that a prototype could feasibly be constructed within the given time with the team's current skill.

### **State-of-the-Art and Emerging Technologies**

Due to the unique nature of this project, there are relatively few new ways of testing the parameters of terrain for micro-class robots. However, one other widely used sensor that is very similar to a bevameter is the Vane-cone device [4]. It follows the same principles as a bevameter, yet instead of using a flat base plate pressed into the terrain to measure these values, it uses conical device (Figure 2). This is plunged into the ground and then spun to obtain both the sinkage and the shear data. For this project, a bevameter was chosen because it more accurately represents a single wheel under load (as a flat surface opposed to a cone).

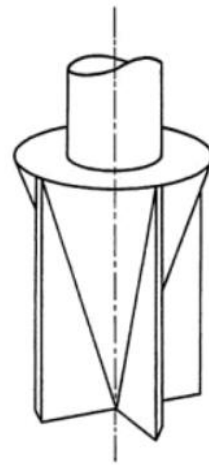


Figure 2: A Vane Cone Device.

Another device called a vacuum bevameter has recently been designed for use on the moon. It measures the lunar soil characteristics within a vacuum chamber at specified temperatures, while also accounting for the much lower lunar gravity [5]. This eliminates most of the

possible outside contaminants and variables to find the most accurate characteristics of the lunar terrain.

## **Generation and Evaluation of Concepts**

Before concepts for the subsystems could be generated, it had to be determined if the bevameter would use two probes – one for each test – or use a single probe to execute both tests. It was discovered that with two separate probes the one that would carry out the shear slippage test would have the same mechanics needed for a single probe system. A single probe bevameter was the chosen design moving forward.

The design for the bevameter was divided into four subsystems:

### **Pressure-Sinkage Design**

The design for this component required an actuator to provide linear motion, an axial load of up to 80 N, as well as provide a constant velocity actuation. Pneumatic, hydraulic and electric linear actuators were considered. A force sensor will be installed in the base plate to measure the force applied throughout testing. There were two concepts that were considered for generating the linear motion to the shaft. One utilized a linear actuator coupled with the shaft which would allow the shaft to be moved and controlled by the actuator. The other concept used a gear motor with a spur gear mounted to the motor shaft that would work with a rack mounted to the shaft to generate the desired linear motion.

## **Shear-Slipage Design**

The design for this component required an additional actuator to provide rotational motion with constant velocity and angular positional control. In order to effectively measure the torque being generated, foil strain gauges will be installed and positioned on the shaft in a Wheatstone bridge configuration, detailed in Appendix I. They will be placed right above the base plate to accommodate for any torque losses throughout the system. There were two methods of transmitting the rotational motion from the gear motor to the shaft. In one, the gear motor would be directly attached to the top of the shaft. The problem with this concept was it significantly increased the complexity of the linear motion because the gear motor would have to move with the shaft. It has to stay connected in order to rotate the shaft. The concept that was selected used a v-belt pulley system very similar to a drill press. The shaft could telescope through the pulley and still accept the rotational motion from the gear motor.

## **Structural Design**

The main factors that were considered when choosing a structural design for the bevameter were the ease of construction, accessibility, portability, and versatility over various terrain (in that order) of the design. There were three different structural configurations that are being considered for the mount or stand. There is a tripod (Figure 2c) with each leg being situated at increments of 120 degrees. There is also a box or rectangular mount (Figure 2a) where the test probes could be situated on the top surface or within the frame and extend downwards towards the ground. The last configuration is a hollow tube (Figure 2b) where the test probes are again situated on the top face or within the tube and plunge through the center to the ground.

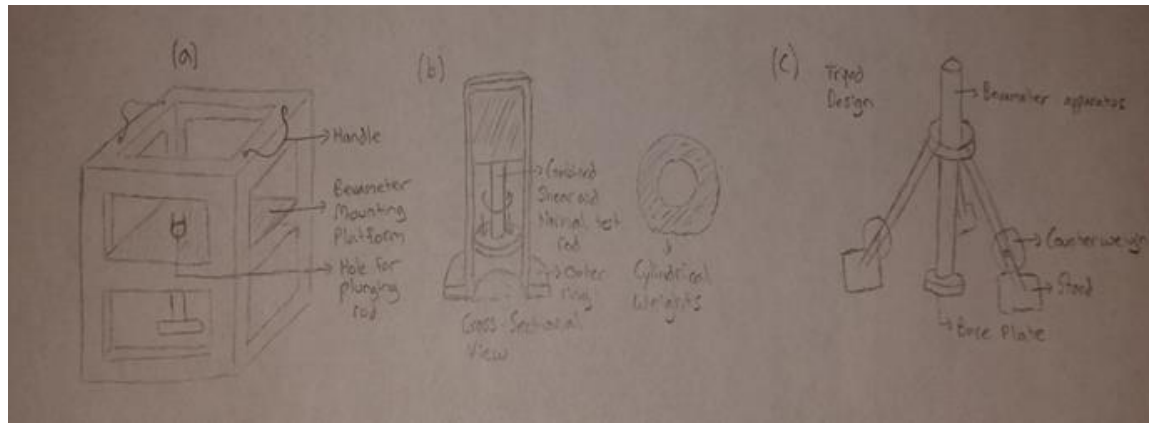


Figure 3: Three structural designs, the cubic casing (a), the cylindrical casing (b) and the tripod design (c).

The box design was selected due to its ease of construction as well accessibility of all components. The tube design, once assembled, would have made for difficult access to the interior components for maintenance or troubleshooting purposes. With the tripod design there were other concerns such as ensuring the frame has enough mass to counter the force being exerted during the test as well as ease of mounting all the necessary components.

### **Microcontroller and UI Design**

The microcontroller selected for the bevameter must have sufficient I/O pins to control the various sensors and actuators as well as have enough processing power to ideally calculate the terramechanics parameters from the data collected. Since the final iteration of the prototype is will be the final product for the customer, it is ideal to also factor in ease of development for the prototyping stage.

Including a user interface is not a requirement of the project, but is something that would be beneficial for the end user. A few concepts were generated, including an LCD screen, phone

app, and blinking lights. Since a UI is based almost solely on qualitative measures, the feasible concepts will need to be tested by volunteers during the full testing stage.

## Engineering Analysis

### Background Mathematics

#### **Pressure-Sinkage Mathematical Model**

To find the pressure-sinkage relationship for a specific wheel size, a flat plate is pressed to a specified depth in a terrain, and the force required to reach that depth is recorded. By repeating this test to various depths, the pressure-sinkage relationship can be plotted. From these plots the Bekker's parameters  $n, k_c$  and  $k_\emptyset$  can be found through the following mathematical process. This process must be performed with at least two different sized base plates for a specific wheel size.

The following equation proposed by Bekker will be used to characterize the pressure-sinkage relationship for the terrain, where  $p$  is the pressure applied,  $z$  is the sinkage and  $b$  is the base plate radius:

$$p = \left( \frac{k_c}{b} + k_\emptyset \right) z^n = k_{eq} z^n \quad (1)$$

Once the experimental data has been collected, a weighted least squares method [4] will be used to derive the parameter values. To do this, first the logarithm of Equation 1 is taken, giving:

$$\ln p = \ln \left( \frac{k_c}{b} + k_\emptyset \right) + n * \ln z \quad (2)$$

A weighting factor  $w_r = p^2$  [4] is then introduced:

$$w_r \left[ \ln p - \ln \left( \frac{k_c}{b} + k_\emptyset \right) - n * \ln z \right]^2 \quad (3)$$

Letting  $k_{eq} = \frac{k_c}{b} + k_\emptyset$ , the equation becomes:

$$\sum p^2 \left[ \ln p - \ln k_{eq} - n * \ln z \right]^2 \quad (4)$$

To find the best fitting values for  $n$  and  $k_{eq}$ , the partial derivatives of Equation 7 with respect to each of the parameters are found, giving:

$$n = \frac{\sum p^2 \sum p^2 \ln p \ln z - \sum p^2 \ln p \sum p^2 \ln z}{\sum p^2 \sum p^2 (\ln z)^2 - (\sum p^2 \ln z)^2} \quad (5)$$

$$\ln k_{eq} = \frac{\sum p^2 \ln p - n \sum p^2 \ln z}{\sum p^2} \quad (6)$$

The value of  $n$  is found as an average of the two  $n$  values calculated (one for each base plate).

$$n_{avg} = \frac{\sum_{i=1}^m n_i}{m} \quad (7)$$

Using this value of  $n_{avg}$ , two values can be calculate for  $k_{eq}$ , one for each base plate test.

With these, the parameters  $k_c$  and  $k_\emptyset$  can be found:

$$k_c = \left( \frac{k_{eq,b1} - k_{eq,b2}}{b_2 - b_1} \right) b_2 b_1 \quad (8)$$

$$k_\emptyset = - \left( \frac{k_{eq,b1} - k_{eq,b2}}{b_2 - b_1} \right) b_2 \quad (9)$$

### **Shear-Slipage Mathematical Model**

The shear-slipage test is performed by pressing a shear ring into the soil and rotating it to various angular positions while measuring the torque output by the motor. The Wong parameters  $c$  (cohesion),  $\emptyset$  (friction angle) and  $K$  (shear deformation parameter) can be calculated using a weighted least squares method once again.

After the experimental data is collected for this test, the stress-shear displacement relationship is plotted. Depending on the type of terrain, this shear curve can end up having three different shapes. If the curve shows a simple exponential form, then the following relationship can be used:

$$\frac{s}{s_{max}} = 1 - \exp\left(-\frac{j}{K}\right) \quad (10)$$

By using the weighted least squares method, taking logarithms and introducing a weighting factor of  $w_r = \left(1 - \frac{s}{s_{max}}\right)^2$ , then the shear deformation parameter can be calculated as:

$$K = -\frac{\sum \left(1 - \frac{s}{s_{max}}\right)^2 j^2}{\sum \left(1 - \frac{s}{s_{max}}\right)^2 j \left(\ln\left(1 - \frac{s}{s_{max}}\right)\right)} \quad (11)$$

However, if the shear curve instead peaks and then shows a continuous decrease as the displacement increases, then the following relationship should be used instead:

$$\frac{s}{s_{max}} = \left(\frac{j}{K_w}\right) \exp\left(1 - \frac{j}{K_w}\right) \quad (12)$$

By following the same procedure once again and introducing a weighting factor of  $w_r = \left(\frac{s}{s_{max}}\right)^2$ , then the shear deformation parameter can be calculated from:

$$\sum \left(\frac{s}{s_{max}}\right)^2 \left[ \ln\left(\frac{s}{s_{max}}\right) - \left(1 + \ln\left(\frac{j}{K_w}\right) - \frac{j}{K_w}\right) \right] [K_w - j] = 0 \quad (13)$$

If the shear curve peaks and then decreases to a constant value as the displacement increases, then the shear deformation parameter can be calculated directly from the following formula:

$$\frac{s}{s_{max}} = K_r \left[ 1 + \left[ \frac{1}{K_r(1-\frac{1}{e})} - 1 \right] \exp\left(1 - \frac{j}{K_r}\right) \left[ 1 - \exp\left(-\frac{j}{K_r}\right) \right] \right] \quad (14)$$

Lastly, the cohesion and friction angle can be found by performing this test under different normal pressures, and using the following Mohr-Coulomb relationship:

$$s_{max} = c + p \tan \phi \quad (15)$$

## Base Plate Analysis

The base plates used for the pressure-sinkage tests performed by the bevameter need to be approximately the same size as the contact area of the wheels on the ground. This contact area depends on the wheel-terrain contact angle  $\theta_c$ , which is shown below (Equation 16). As you seen in Figure 4, the contact angle depends on the depth to which the wheel sinks into the soil, which is dependent on the type of soil that the bevameter is testing.

$$A = r_w w_w \theta_c \quad (16)$$

$$\theta_c = \cos^{-1}(1 - z/r) \quad (17)$$

$$z = \left[ \frac{3F}{(b\sqrt{2r}(3-n)\left(k_\phi + \frac{k_c}{b}\right)} \right]^{\frac{2}{2n+1}} \quad (18)$$

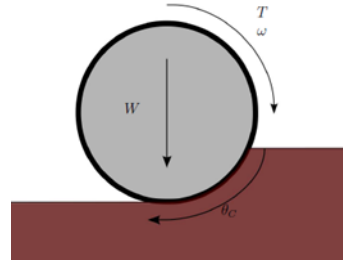


Figure 4: Diagram of rigid wheel in contact with terrain.  $W$  is the weight on the wheels;  $T$  is the torque driving the wheels;  $w$  is the rotational velocity of the wheel;  $\theta_C$  is the wheel-terrain contact angle. [2]

Therefore, to find suitable base plate areas, a few common soils that encompass the range of terrain that will be experimented on in the future were chosen (LETE Sand, Sandy Loam, and Clayey Loam). Using average values for the Bekker's parameters for these specific soils as reported by Wong (Table 2), and with the given maximum 80 N single wheel load, the depth  $z$  can be estimated using Equation 18. The contact area of the wheels can then be calculated, and thus the base plate radii can be found (Table 3).

Table 2: Bekker's parameters for LETE Sand, Sandy and Clayey Loam as reported by Wong [4].

Parameter		LETE Sand	Sandy Loam	Clayey Loam
$k_c$	Soil modulus of cohesion	1.16	3.3	6.8
$k_\phi$	Soil modulus of friction	475	2529	1131
$n$	Soil deformation exponent	0.611	0.850	0.850

Table 3: Base plate radii for desired wheel sizes calculated for various soil types (See Appendix VI for calculations).

Wheel Size		Base Plate Radii (cm)		
Width (cm)	Diameter (cm)	LETE Sand	Sandy Loam	Clayey Loam
5	10	6.4	<b>5.7</b>	<b>6.6</b>
7.5	15	7.6	<b>6.9</b>	<b>8.0</b>
10	20	8.5	<b>7.9</b>	<b>9.2</b>

Two base plates are needed to solve for the Bekker's parameters of the terrain for a specific sized wheel. Therefore the smallest and largest of the three base plate radii calculated for each wheel will be used (bolded in Table 3).

### **Base Plate Design**

The base plate design consisted of two parts that were connected with four screws. The shaft penetrates the top piece and uses a shaft collar to ensure the base plate does not slide off the shaft. The top piece also has a shaft key printed into it to allow the base plate to rotate during the shear slippage test. It then fits inside the bottom part of the base plate, there are four holes put in the side of each piece so when coupled together they can be secured with screws. Having the base plate secured with screws allowed for the base plates to be easily interchangeable, as per the project requirements. There is a cylindrical pocket between the two components which is where the force sensor is situated. The shaft will make contact with the force sensor when the linear actuator is driving the shaft downward allowing for the force being exerted to be monitored.

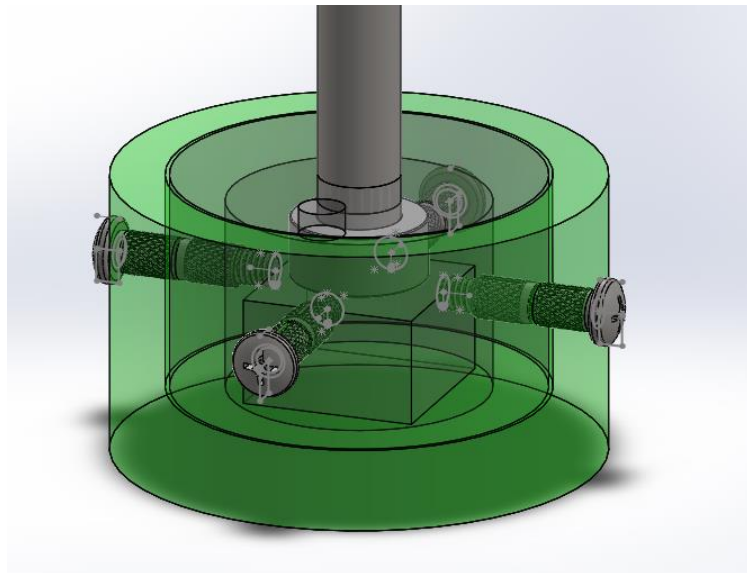


Figure 5: Final base plate design mounted on shaft.

After some deliberation, it was decided that these would be 3D printed using the on campus MakerBots to save both the money and time it would have taken to make them out of a stronger material (ie, steel). It also removes the risk of ruining the component while manufacturing by a student. Based on a Finite Element Analysis run, the plastic used is able to withstand the 80 N reaction force and 4.8 N-m torque that it will tested under, however the base plates will likely wear down much faster under repeated test loads than a base plate made of steel would. This was found to be acceptable for prototyping purposes. A goal was also set at the beginning of this project that required there to be six different sized base plates to test three different wheel configurations for the pressure-sinkage test, however, for proof of concept and testing, only two are necessary and so only one set was printed. One additional base plate will be printed with grousers on the bottom surface to perform the shear-slippage test.

## **Refinement of Design**

There were four material choices available for the main shaft from McMaster-Carr. Since the shaft is one of the main components of the bevameter and will undergo all of the applied forces of the two tests, a cost, buckling, and elastic deflection analysis was conducted in Appendix III. From this, it was found that the standard 1045 steel shaft was the best candidate. A second material and cost analysis was conducted for the available hollow rectangular tubing to be used for the structural frame in Appendix IV, and it was found that the cheapest solution of 1020 carbon steel was adequate for this application.

### ***Design One***

The structural design chosen was the rigid prismatic frame. The structure consists of a box frame with a flat platform that all components will be mounted to. With this configuration, the structure can resist reaction forces that are produced during the tests as well as the resultant torque. An additional platform will be added which will be driven up and down by an electric linear drive. The gear motor will be mounted on the top of this platform. There will be a hole through this platform that will allow for the motor and the shaft to be connected through a shaft couple. To ensure the top platform that houses the gear motor moves vertically – and does not sway and twist during operation – metal rods have been added as guide rails. Since budget is a big constraint with this project, plastic tubes will be added to assist in ensuring the guide rails do not get seized up, and to keep the top platform properly aligned. Ideally linear bearings would be used instead of the tubes – but they are neither cost effective nor essential to the design.

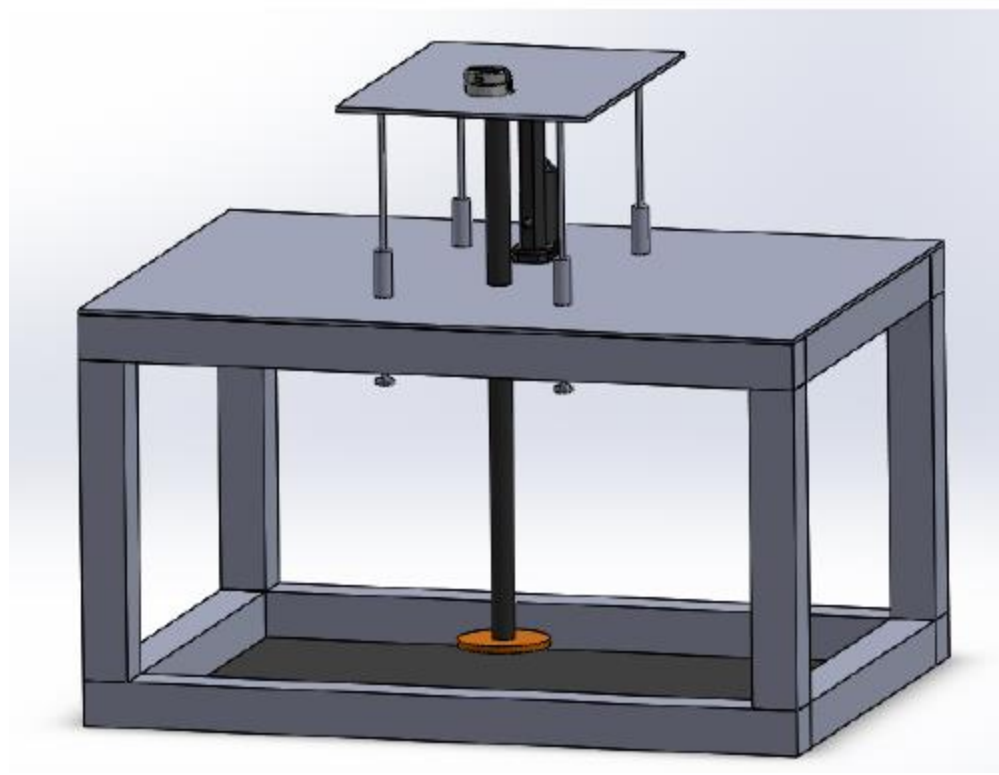


Figure 6: SolidWorks model of initial design.

#### ***Design One Refinement***

Before moving on to the design analysis stage of this project, a number of problems with the original design were addressed and a few small improvements were made. One of the biggest problems with the original design was that it was too heavy to take out into the field. To fix this, the solid rectangular beams used for the structural support were exchanged for hollowed rectangular tubes. This, along with a few other changes, brought the total mass down to 16.3 kg, which was right in the mass range constraint of 10 – 20 kg. The height of the structural components was also reduced by over half. Not only did this reduce the mass, but it reduced the required length of the shaft – which will decrease the bending in the shaft when the compressive load in the pressure-sinkage test is applied to it.

The position of the linear actuator with respect to the shaft was the next thing to be changed. It was centered on the frame and moved closer to the shaft in order to reduce the tilt on the shaft caused by the actuator. A flange-mounted bearing was added to the shaft at the top plate to keep the shaft aligned and allow it to move linearly and rotate freely. Finally, the motor used to perform the rotational motion of the shaft was changed, since the original gear motor couldn't provide enough torque to perform the shear-slipage test. A larger compact AC gear motor was chosen, which is more expensive but can cover the maximum expected torque of 4.8 Nm. The design was as follows:

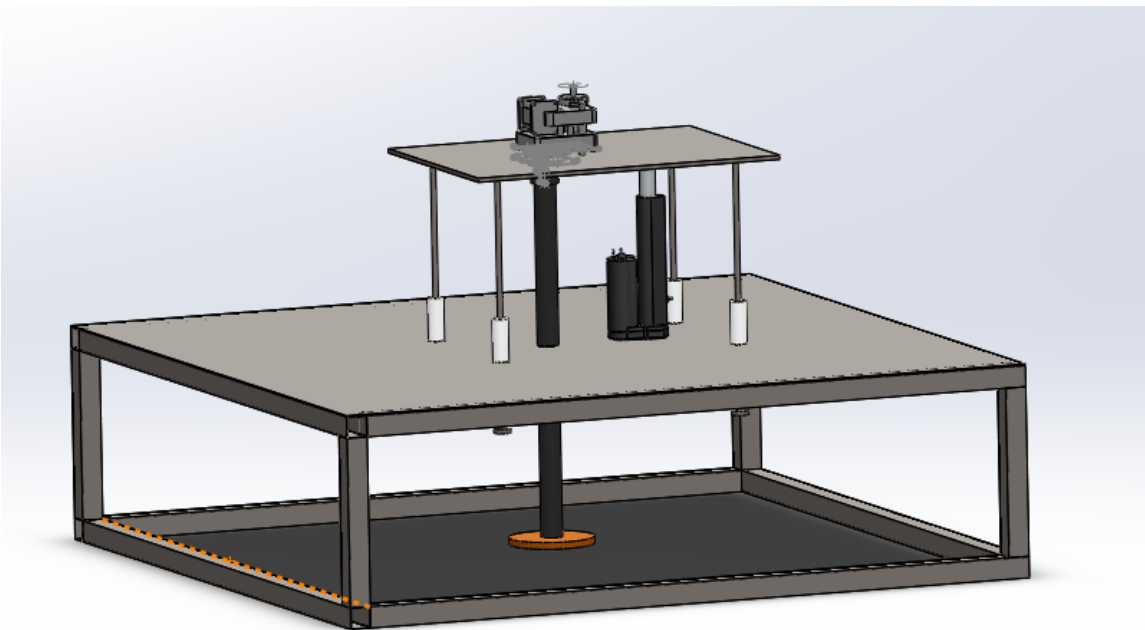


Figure 7: SolidWorks model of design one following the first round of iterations.

### ***FEA of Design One***

A finite element analysis (FEA) was done on the structural and mechanical components of the bevameter. The worst case scenario – conducting the shear-slipage test under the maximum load and maximum torque – was tested. First, the structural rectangular tubing was made into shell components with a 0.76 mm thickness. After shelling those components, contact sets needed to be applied between the shelled and solid parts. Gravity was applied to the system, which has a mass of 16.3 kg. The frame was fixed at the bottom (ground), and the base plate was fixed to resist the rotational motion and the applied force downwards of the worst case scenario for the shear-slipage test.

An 80 N force was applied to where the linear actuator would be attached to the top plate to simulate the maximum pressure that could be used to push the base plate into the ground. A 4.8 N-m torque was applied on the shaft to simulate the worst case expected torque during the shear-slipage test. The model was then meshed with a mesh size of 18.07 mm (lower sizes from the default caused the system to crash). The results from the FEA can be seen below:

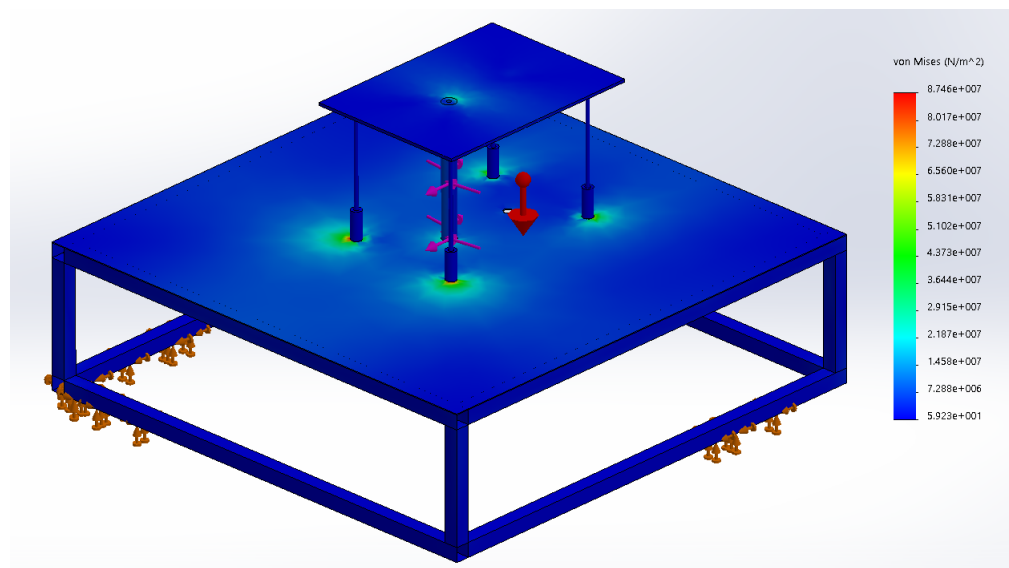


Figure 8: FEA static nodal stress plot of design one.

From the above plot it can be seen that there are large stress concentrations focused around where the guide rails meet the top of the frame. This is further highlighted in the figure below, which is a zoomed view of the displacement plot created during the analysis.

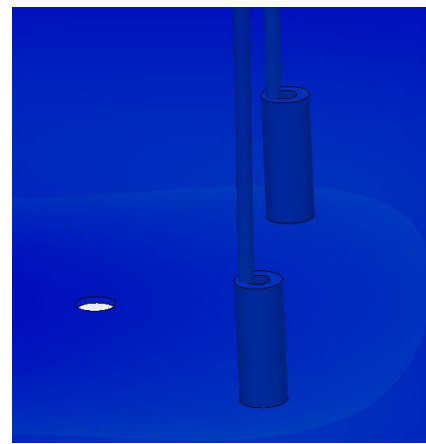


Figure 9: FEA static nodal displacement plot of design one, focused on the guide rails.

There is some tilt and displacement in the guide rails where they meet the top of the frame, which in practice will mean that the guide rails will most likely seize up during the testing phase. This points to a fundamental flaw in this design of the bevameter. To fix this, significant changes needed to be made to the design.

### **Design Two**

Due to the fundamental flaws found in the analysis of the previous design concept, it was necessary to look at alternative solutions. The best solution was one that utilizes the same mechanics as a drill press. The concept consists of a main operating shaft that must rotate as well as move in the vertical direction – which are the exact movements a standard drill press is designed to have. With this design, the top plate is fixed, therefore eliminating the seizing issue that arose in the previous designs which utilized guide rails to move the entire top plate and all the components attached to it.

As a result of the new design, the motors and sensors had to change position as well. The gear motor being used for the shear slippage test was relatively easy to reposition. Its shaft had to be concentric with the through hole of the adjustable speed v-belt pulleys. In addition, the motor is face mounting, which allows it to be fixed directly to the top plate which minimizes the distance the rotary motion needs to be transferred. The gear motor will have to be coupled with an additional shaft which will extend through the pulley.

The system that will be generating the vertical motion in this concept is more complex, but can still execute the necessary tasks. The linear mechanism consists of two shaft collars, two ball bearings, and a steel mounted ball bearing (Figure 10). There is also a motor that is

attached to a spur gear which is the pinion of the system. The mounted ball bearing is attached to a small piece of sheet metal that has the rack mounted to the opposite side.

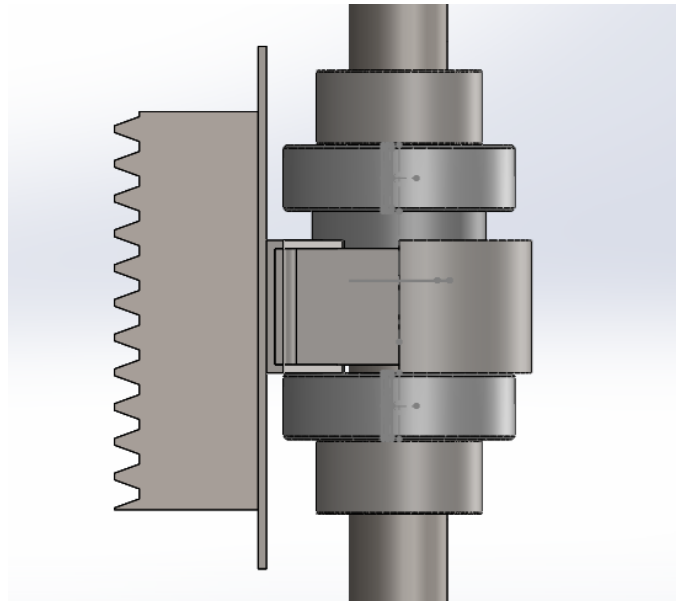


Figure 10: Linear Mechanism on Shaft (Top down: Shaft Collar, Ball Bearing, Mounted Ball Bearing, Ball Bearing, and Shaft Collar).

The last part of the design that had to be considered and reevaluated was the structural frame of the bevameter and positioning of all the parts coming together into one device. The first problem with the frame from the original design was the excessive size – and the resulting mass. One of the objectives for this project was to make the bevameter untethered and portable, so that the user could easily transport the device to and around the testing site. By decreasing the size of the frame from 85.5cm x 85.5cm x 25.1cm to 42.5cm x 42.5cm x 25.1cm, the mass decreased from 9.75 kg to 4.5 kg. This new frame can easily be carried by an individual, as well as the reduced size of the frame will make it easier for the user to handle the device. It also helps to keep the project costs down – less material is needed for the smaller frame. Due to the decreased weight, extra mass will need to be added to ensure the device

does not move or shift during operation. The last thing that needed to stay constant with the new design was that the test probe is centered within the frame. This is to decrease any disturbances that may arise in the soil due to the close proximity of the frame to the soil being tested.

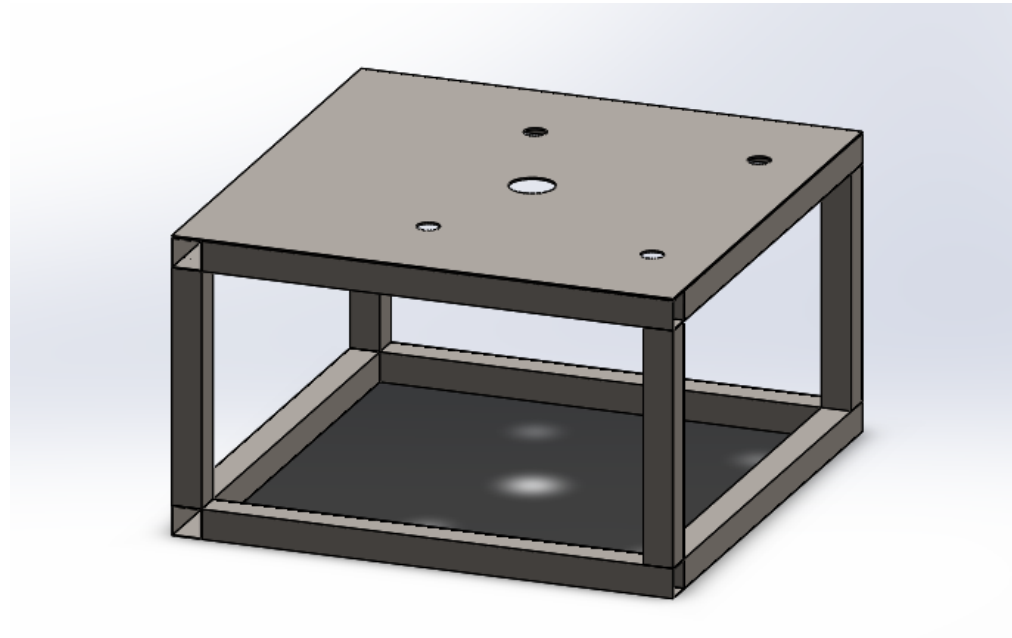


Figure 11: Reduced size of structural frame.

#### ***FEA of Design Two***

Before running the FEA simulation on the design, the situation that needed to be evaluated and analyzed had to be described. The situation chosen to focus on was when the bevameter was performing the shear slippage test – this has both the force driving the shaft and base plate down as well as the torque being generated from the shaft rotating.

An 80 N force was added in the downward direction on the shaft. The torque was then added to the top of the shaft, since this is where the rotary motion is being transferred to the shaft from the gear motor. In addition to adding the forces and torques to the model, fixtures needed to be added. The bottom face of the frame was fixed, to mimic the test – where it will be resting on the ground with enough mass (over 10 kg) that it will not move due to the resulting forces. The last thing needed before running the simulation was defining the frame supports as shells since they are thin walled rectangular tubes. The mesh size that was used for this simulation was the default size of 13.91mm.

The simulation was then run and the displacement and stress plots analyzed. As seen in the figure below (Figure 12) there was an applied downward force of 80 N on the shaft in addition to a 4.8 Nm torque. The maximum displacement was as expected and occurs at the top of the shaft, which is a result of it being the farthest point on the shaft from where the force is being applied. The largest displacement is still very small, at  $2.663 \times 10^{-1}$  mm. The end of the shaft (with the expected largest displacements) will be positioned through the adjustable speed v-belt pulley which will aid in maintaining proper alignment of the shaft at all times during operation. In addition, there are no unexpected stress concentrations in the system. The highest stress occurs in the mounted bearing. Since the force is acting on a slight angle, it is generating some stress and bending in the mount. These stresses aren't expected to be an issue. Another area of higher stress is at the bottom of the shaft, around the connection to the base plate. This is acceptable for our design since we are measuring the force at this point. From this FEA analysis we can see that with the new design we avoid stress concentrations that would result in failure of the bevameter.

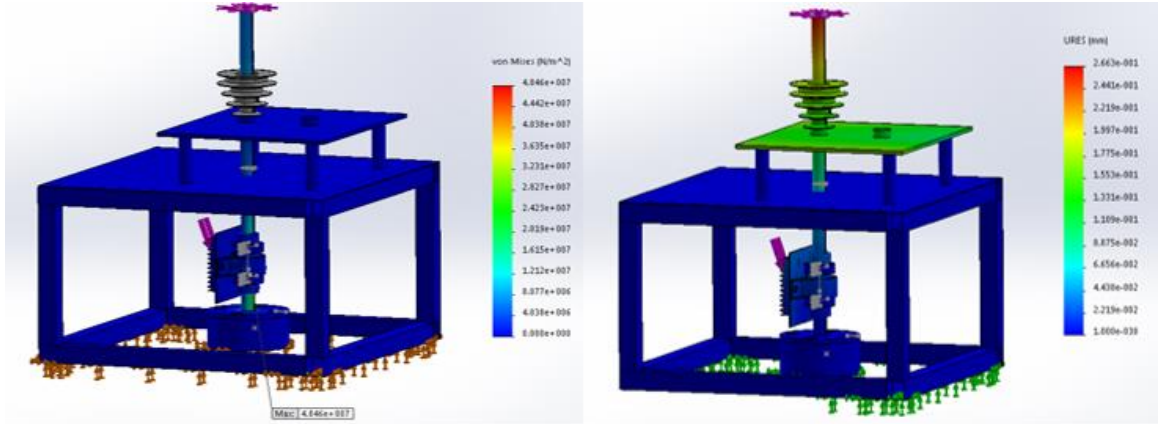


Figure 12: FEA of final design, Von Mises (left) and Displacement (right)

## Final Design

The previous design seemed to be sufficient through our analysis, however the complexity of the linear actuation design combined with the small margin for error with the gear track components made it a high risk solution. With the limited time and resources given for prototyping, the feasibility of this design was in question. After seeking the advice of an experienced professional, further iterations were considered leading to the following final design, which combined aspects of the previous two designs in order to minimize the prototype complexity while maintaining the benefits of the previous design.

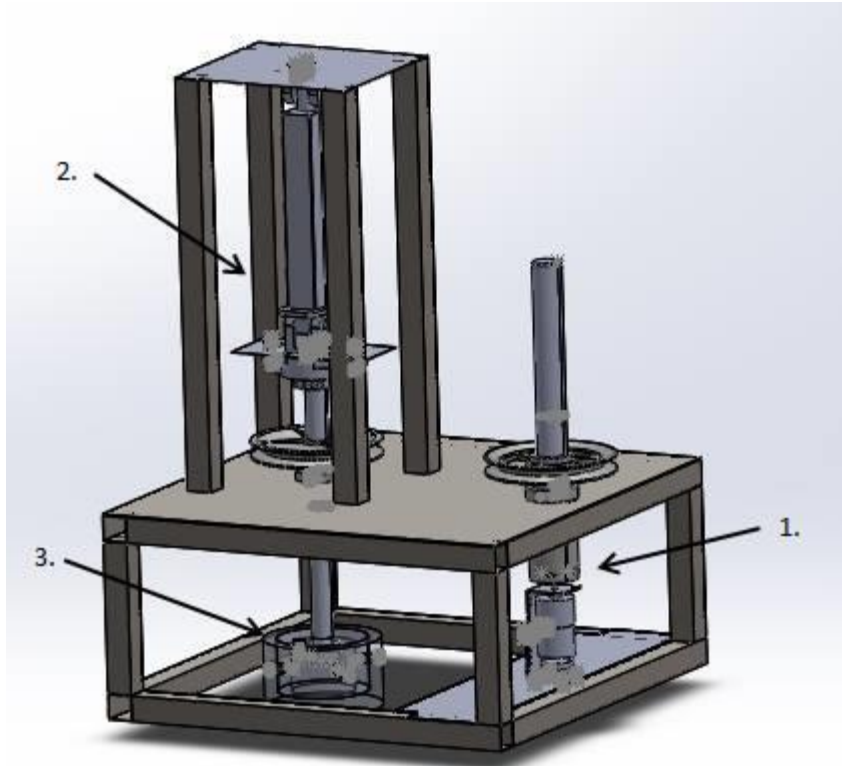


Figure 13: Final prototype design. 1. Base plate. 2. Linear actuator design. 3. Gearmotor assembly.

The entire purpose of this design project was to build a fully-functioning, to scale prototype of a micro-bevameter. With this in mind, the feasibility of the project in terms of cost, skill and time was at the forefront of every step of the design process. The final design shown above contains all of the components and materials that will be used to produce a functioning prototype to assess the core functionality of the design. Complete part and assembly drawings can be found in Appendix IX. Many of the components in that design were not chosen because they were the ideal part for the design, but rather because they were cost effective and could still produce adequate results. The following sections will break down exactly what concessions were made during the design process in order to feasibly construct a working prototype.

### ***Sensor and Actuator Selection***

Two actuators were needed to produce the rotational and linear motions on the shaft that are required to conduct the two experiments (pressure-sinkage and shear-slippage tests) that the bevameter is designed for. For the linear motion, the gear track system from the second design was replaced, as previously mentioned. It was decided that a linear actuator would be used that met the requirements (FoS of 2) and attached to the shaft. It would still produce the same motion and force however it was also more expensive, so in simplifying the design and saving time during the prototype construction, money was lost. In addition to that, the overall size of the design had to be increased in order to incorporate the linear actuator properly.

The second actuator, used to produce the shaft's rotational motion, needed to be able to maintain a constant angular velocity under an increasing torque load, so a gear motor was chosen. It also needed to be able to rotate in both directions to prevent the wires of the sensors mounted to the shaft from becoming too tangled (solutions to this problem, such as slip rings, were too expensive for the prototype), which meant that the motor needed to be DC. Balancing both cost and the motors constraints (170 oz-in stall torque), a motor was chosen with a 250 oz-in stall, which didn't meet the ideal factor of safety of 2 chosen for the design, but was fairly cheap and easy to install.

To perform the pressure-sinkage test, two readings need to be taken; the force being applied to the ground by the linear actuator, and the linear displacement of the shaft in the direction of the force. The obvious choice for reading the applied force of the shaft was to use a compression load cell, however these averaged around \$80 for cells that could read up to the required 80 N, which was too expensive. Instead, a cheap weight scale was disassembled and

the load cells within were appropriated for the prototype. The trade off in this case was a loss in precision, however precision isn't critical for the later calculations with regard to the force so it was tolerable. To find the displacement of the shaft, ideally a separate linear encoder would have been used to reduce any error caused by backlash in the linear actuator, etc. Once again there were budgeting issues, and it was significantly cheaper to purchase a linear actuator with an internal potentiometer than it was to purchase a separate actuator and sensor as well as their respective mounting components.

The same expense issues were run into once again when considering sensors for the shear-slippage test, where the torque on the shaft and the angular displacement of the shaft must be found. To reduce costs, a DC gear motor with an internal encoder was chosen, when ideally an external encoder would have been used. Foil strain gauges can be used to measure the torque on the shaft. The cost was not ideal, but the gauges are necessary, and they are quick to configure and calibrate so they were chosen for this prototype.

### ***Mechanical Components***

As stated earlier, the final design contains all of the mechanical components and materials that will be used to produce a fully functioning prototype, even if these aren't always the most ideal choice for the design. One of the biggest concessions that was made with respect to this was the material and manufacturing process that will be used for the custom designed base plate components, as detailed previously in the base plate design section.

Another problem encountered was that the largest DC gear motor output shaft diameter available within the project budget was  $\frac{1}{4}$ ", while the smallest keyed borehole size for the V-

Belt pulleys being used to transfer the rotational motion was  $3/8"$ . The ideal solution of using a shaft adapter to connect the two shafts was too expensive as well, so a makeshift solution using a shaft coupler and mounting hub was created. There will be some torque loss across this coupling, however, since the torque will be measured right near the base plate, the losses will not affect the measurements being taken. Finally, ideally the main shaft would have been made of a lighter material than steel, such as aluminum, to reduce the stress on the linear actuator as it has the weight of the shaft on it, but again, anything other than steel was also significantly more expensive.

#### ***FEA of Final Design***

Finite element analysis was done to the final design and specifically to the shaft and base plate component since this was the main part of the design which had to handle compressive and torsional loads. The first analysis that was done was a simulation of the pressure sinkage test (Figure 14). The desired force of 80 N was applied to the top of the shaft since this is where the linear actuator is acting when driving the shaft. The bottom of the base plate was then fixed to represent the base plate being depressed into the ground during the test. The results were as expected, even smaller displacement than design two was seen in addition to the stress concentration being at the force sensor.

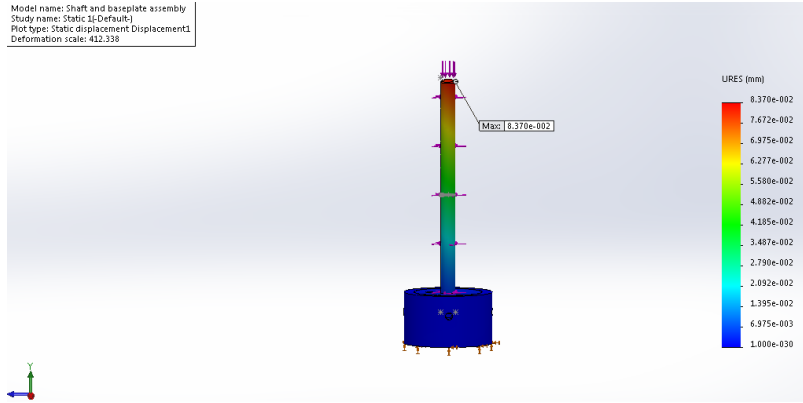


Figure 14: FEA pressure sinkage

The second analysis was done to test the shaft and base plate against the forces of the shear slippage test (figure 15). The only thing that changed from the first finite element analysis was we added the expected torque to the shaft. The base plate was still fixed to represent the worst case scenario during the test. For example if the bevameter was testing very hard soil such as clay the base plate may not be able to rotate with the torque being provided. With this simulation we still saw a very small displacement as well as no unexpected stress concentrations.

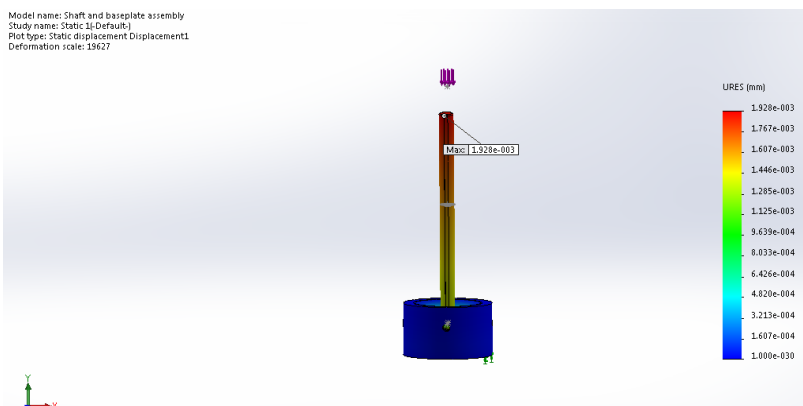


Figure 15: Shear slippage test

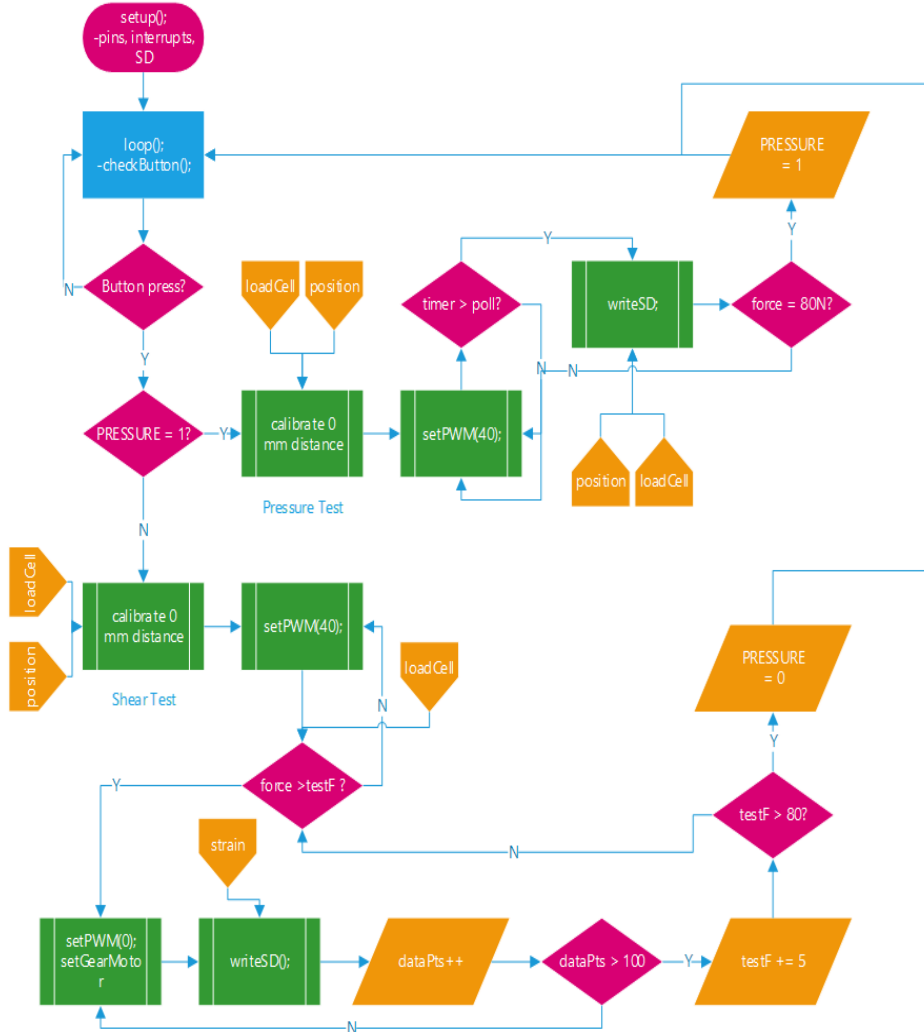
## **Control System**

Selecting the processing device for the bevameter was done to optimize several factors. The first was the requirement that the prototype be as minimally complex as possible – this means a platform that the team has had previous experience on. The development stage also required a processing device that facilitated quick reprogramming for debugging the circuit and code. The requirements, as given by the supervisor, stated that at minimum the device needed to record the raw data from the tests for post-processing; therefore, the microprocessor needed to have the ability to write and save data to an external source. This same requirement stated that ideally the device would calculate the parameters onboard, so the choice needed to have enough processing power to handle the maths, as well as a platform that the student and/or team who will be taking over is likely to know, or can learn how to use quickly. Since the chosen motors for the design require a 12V battery, power was not a deciding factor for this subsection.

Once the monetary constraint was factored in, it was obvious that the Intel Galileo purchased last summer for this project was ideal. The microprocessor coded like an Arduino, allowed for Linux firmware calls, and is based on Intel architecture. Using this microprocessor took no money out of the budget, and the Galileo has 12 digital I/O pins, and the 6 analog I/O pins have a 12 bit resolution. This covers the required pins for the current sensors and actuators, while leaving space for the additional sensors required for measuring the base plate angle. The Galileo also has an onboard microSD slot that holds up to 32 GB, as well as various ports (USB, mini-PCI Express, Ethernet, etc.) that can be used for future improvements.

The data collected by the microprocessor will be saved onto a microSD card, which can then be transferred onto a laptop for post-processing using MATLAB (Appendix VII). The control system was designed such that the user could use a single button to operate the bevameter.

The final control system design is as follows:



16: Control system flow chart

The electrical system designed for these components was developed into a shield for the Intel Galileo, and the part files are ready to be sent off for fabrication.

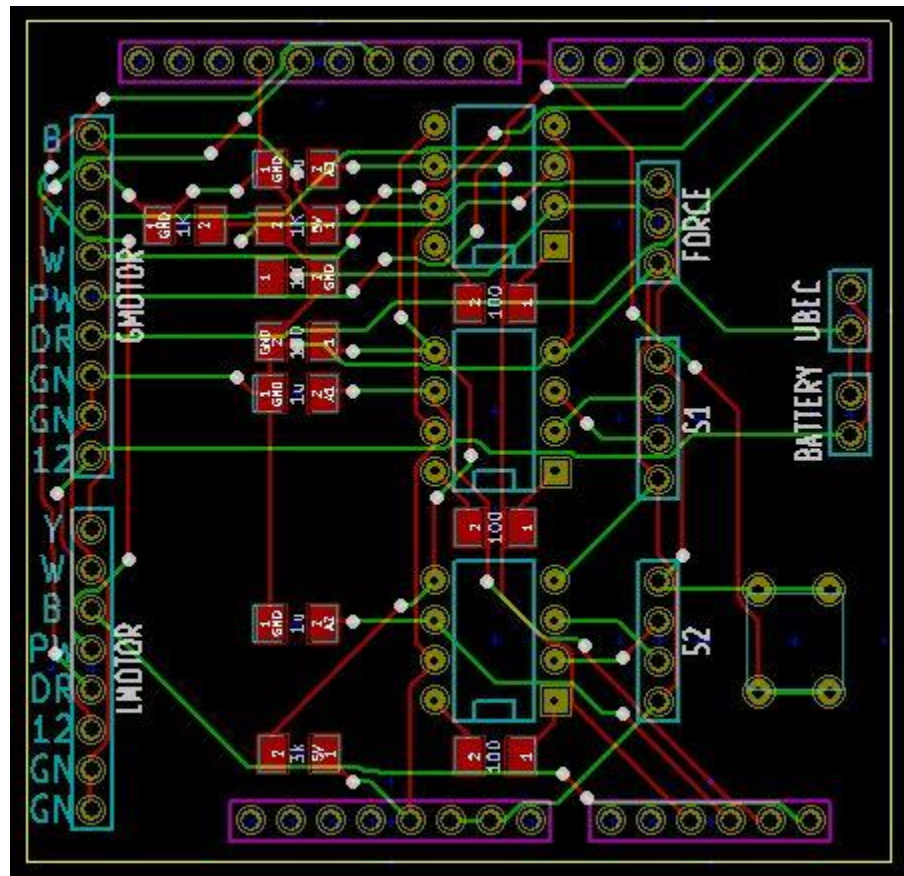


Figure 17: PCB design for an Intel Galileo shield

## **Prototype Development**

### **Prototype Construction**

When constructing the prototype the frame needed to be assembled first since it was going to support most of the other components. The first part of the frame that was built was the very bottom rectangular prism. Two six foot long tubes were purchased for this part, and they had to be cut down to size using a horizontal band saw. Ideally they would have all been secured together by welding, but due to the lack of training and time to learn, it was decided to assemble the frame using L-brackets, screws and nuts. This resulted in over 100 holes being measured, marked and then machined using a drill press. The placement of the holes were crucial to the development of the prototype, because if they were not in the correct location, the L-brackets would not align with the holes. If the holes were out of position, other measures would have been considered to correct this, but luckily this problem was not encountered.

Once this was assembled, the top plate of sheet metal was cut to size using a shear, and the necessary holes for mounting were added with the drill press. The holes for the two shafts to pass through had to also be added at this stage. A punch was utilized for this task, since the size of the holes (3/4", 1") needed were too large to drill into a thin piece of sheet metal. The piece of sheet metal was then secured to the frame using screws and nuts.



Figure 18: Prototype with all components.

The top platform which the linear actuator was mounted to was the last part of the frame to be assembled. Tubes had to once again be cut down to size as well as have the appropriate holes drilled for the L-brackets. Once the bars and top piece of sheet metal were assembled it was mounted to the piece of sheet metal previously discussed with L-brackets. The linear actuator mount was secured to the top piece of sheet metal which allowed the linear actuator to hang underneath the top platform and drive the shaft up and down. The linear drive mount had to be

situated directly above the hole that was punched in the sheet metal so the shaft and linear drive could remain vertical.



Figure 19: Linear actuator coupled with main shaft.

Once the frame was fully assembled, all the other components could be installed. The final pieces that had to be sized were the shafts and shaft keys, which were machined using the horizontal band saw and a sander. The gear motor was first component added to the structure. It was then coupled with the one inch shaft which had one of the v-belt pulleys secured to it. The linear drive was then connected to its mounting bracket that was previously installed, it could then be coupled to the main shaft with the flanged concentric bearing mechanism that

was put together. The second v-belt pulley was placed over the other shaft prior to coupling with the linear drive. The v-belt and base plate were the final components added. The prototype could execute the necessary movements for the two tests but does not have the sensors necessary installed yet.

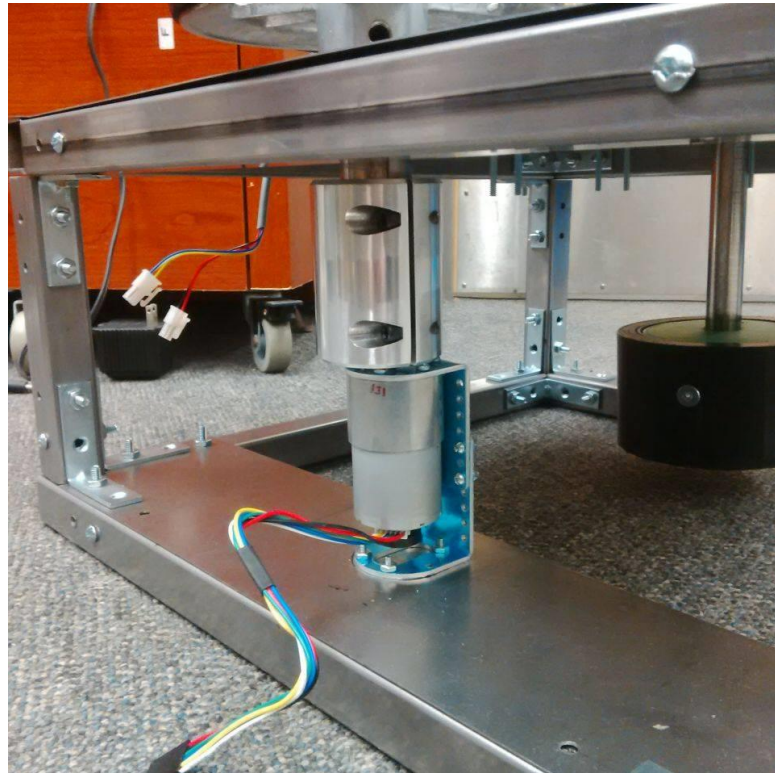


Figure 20: Gearmotor coupled to shaft.

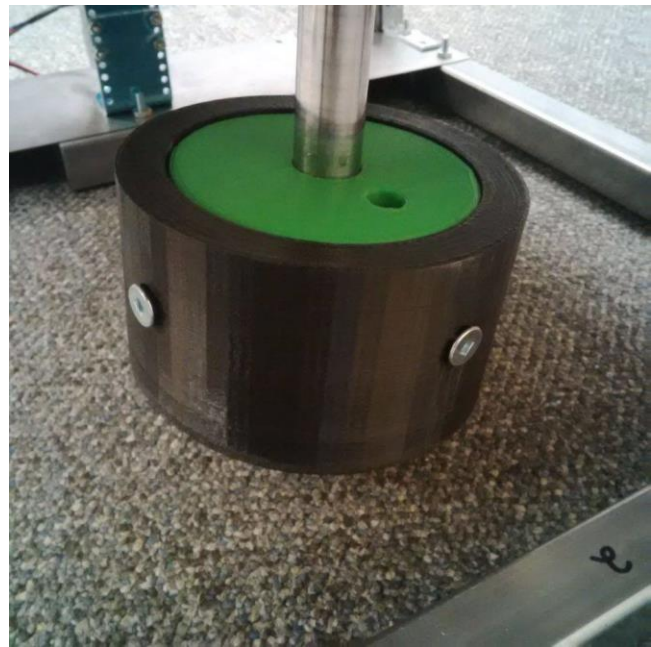


Figure 21: Base plate assembly.

## Budget

This project started out with a budget of \$300. However, after spending a significant amount of time designing and redesigning the prototype, our group found that it was impossible to build a prototype that met all of the given constraints within the given budget. The sensors and actuators necessary to get usable data alone totaled nearly \$300. After contacting the project supervisor, the budget for the project was increased to allow the parts needed to be purchased in order to construct the prototype. The following table details all of the components needed for the prototype, including their description, part number, price, the number of items needed and where they were purchased from.

Table 4: Cost breakdown of mechanical and electrical components.

Component	Part Number	Purchased From	Price (\$)	Number of Items	Comments
<b>Mechanical Components</b>					
Fully Keyed 1045 Steel Drive Shaft	1497K161	McMaster-Carr	21.2	1	3/4" OD, 3/16" Keyway Width, 12" Length
Fully Keyed 1045 Steel Drive Shaft	1497K281	McMaster-Carr	27.6	1	1" OD, 1/4" Keyway Width, 12" Length
Spring Steel Standard Key Stock	98535A140	McMaster-Carr	2.77	1	3/16 x 3/16, 12"
Spring Steel Standard Key Stock	98535A150	McMaster-Carr	3.7	1	1/4" x 1/4", 12" Length
Set Screw Shaft Collar	9414T15	McMaster-Carr	1.97	1	3/4"
Steel Ball Bearing	6383K49	McMaster-Carr	7.48	1	3/4" hole diameter, Pulley support
Steel Ball Bearing	6383K57	McMaster-Carr	12.04	1	1" hole diameter, Pulley support
Two-Piece Clamp-on Rigid Shaft Coupling	6115K15	McMaster-Carr	20.11	1	1" x 1" Diameter Shaft, Aluminum
Zinc V-Belt Pulleys for a-	6245K72	McMaster-	15.5	1	3/4" Bore Size

section Belts, 5" OD		Carr			
Zinc V-Belt Pulleys for a-section Belts, 5" OD	6245K72	McMaster-Carr	15.5	1	1" Bore Size
A-Section V-Belt	6186K133	McMaster-Carr	9.03	1	36" Outer Circle
Sheet Metal 24 x 24	6544K15	McMaster-Carr	14.39	1	Top Plates
Rectangular tubes 6ft	6527K134	McMaster-Carr	8.72	4	Structural Beams
Rectangular tubes 1ft	6527K134	McMaster-Carr	2.88	1	Structural Beams
Browning Normal-Duty Flange Unit	VF2B-212	Amazon Supply	18.57	1	2 Bolt, BOA Concentric Lock
Mounting Bracket for Concentric LD Linear Actuators	2314	Pololu	12.95	2	Need one for each end of actuator
Stamped Aluminum L-Bracket Pair	1084	Pololu	7.95	1	For 37D mm Metal Gearmotors
Universal Aluminum Mounting Hub	1083	Pololu	7.95	1	For 6mm Shaft, #4-40 Holes (2-Pack)
Base Plates	N/A	3D Printed	0	2	Custom Design
<b>Electrical Components</b>					
Concentric LACT4P-12V-5 Linear Actuator	2319	Pololu (US)	109.95	1	4" Stroke, 12V, 1.7"/s, with Feedback
131:1 Metal Gearmotor 37Dx57L mm	1447	Pololu (US)	39.95	1	With 64 CPR Encoder
Compression Load Cell	N/A	Target	31.99	1	Weight Scale, came with 4
Strain Gauges	SGD-3/350-LY11	Omega	68.00	1	Packs of 10 only
Intel Galileo	N/A	Donated	0	1	Donated by faculty
Motor Controller - MD10C	RB-Cyt-132	Robot Shop	0	2	Salvaged from LunaTron's old system
<b>Total Cost</b>			<b>499.31</b>		

## **Testing and Evaluation**

The initial testing phase proved that the actuators could be controlled as in the device code (found in Appendix VIII), and that these actuators could produce the required movements for the two tests. Code snippets were tested as development occurred up to the point where the strain sensors were needed.

The project was unable to move forward with the full testing phase of the design due to a couple of small but critical issues, both having to do with sensors chosen for the design. The first was that the strain gauges took significantly longer than expected to arrive from the manufacturer, not arriving until days after the design showcase was held. The second was that the load cells used for the design needed to be amplified more than was expected, causing issues of precision since the voltage range during testing fell between 0.996V and 1V when applying loads between 0 and 80N.

To test this prototype, a number of modifications would need to first be made. These are detailed in the following section, modifications and improvements. To perform the pressure-sinkage test, first the smaller, flat-bottomed base plate should be attached to the main shaft. The prototype should then be moved in to position and the code for the pressure-sinkage test should be run by pressing the button on the Galileo shield; the resulting pressure and displacement data will be saved in a file named “PressureTest.txt”. When finished, the smaller base plate should be exchanged for the second, larger flat base plate. The prototype should be shifted to a new, undisturbed soil patch, and the pressure-sinkage test will then be rerun by pressing the button again. To perform the shear-slippage test, the flat base plate should be

exchanged for the base plate with the grousers on the bottom. The shear-slipage test should then be run twice, in the same manner as the pressure-sinkage test, with this base plate, once at a pressure of 20N and once at a pressure of 40N. The prototype should again be shifted to another position between the tests to avoid testing on disturbed soil. This data can be post-processed on a computer with MATLAB using the script in Appendix VII, and then compared against the expected parameters for the type of soil tested.

## **Modifications and Improvements**

There are a number of modifications that should be made to the prototype in order to move forward with the testing phase of the design. The biggest of these is the installation of the strain gauges, without which the torque readings for the shear-slipage test cannot be read. The layout of these on the shaft is detailed in Appendix I. The load cell housed in the base plates used for the two tests needs to be amplified using the designed PCB. A linear bearing should also be purchased and attached to the prototype's main plate to help guide the main shaft (3/4"), since presently there is too much play with how the shaft can tilt out of place. A 12V power supply is necessary in order to be able to test this device outside of a lab setting. Finally, a micro-SD card needs to be purchased in order to be able to save the data collected during any of the tests.

Along with the previously mentioned modifications, a few improvements could also be made to the design. Rather than using a breadboard to hold part of the designed circuit, a PCB should be used, which is detailed in Appendix V. All of the provided code, from the data collection code to the parameter calculation could be improved as needed, since they were

unable to be properly tested during the testing phase of this project. Finally, visual encoding could be used on the base plate or main shaft itself to account for any slip, rather than relying on the internal encoder of the gear motor to provide accurate data.

## **Project Planning and Scheduling**

As can be seen in the table below, the original task list and schedule changed throughout the project lifespan. This was due to a number of tasks taking significantly longer than originally expected. These included the design iteration and refinement process, the actuator and sensor selection process and the prototype construction. The Gantt chart detailing the original task list and schedule can be found in Appendix II.

Table 5: Table of tasks and deliverables, including the original estimated hours and dates, and the final actual hours and dates spent on the tasks.

<b>Tasks/Deliverables</b>	<b>Estimated Hours</b>	<b>Estimated Calendar Dates</b>	<b>Actual Hours</b>	<b>Actual Calendar Dates</b>
Project Proposal	6	Sep. 24, 2014	Sep. 29, 2014	3 Sep. 24, 2014 Sep. 29, 2014
Terramechanics Research	10	Sep. 24, 2014	Oct. 3, 2014	10 Sep. 24, 2014 Oct. 3, 2014
Calibrate Existing Rover Sensors	4	Oct. 3, 2014	Oct. 6, 2014	5 Oct. 3, 2014 Apr. 8, 2015
Pressure/Sinkage Concept Design	5	Oct. 6, 2014	Oct. 15, 2014	5 Oct. 6, 2014 Oct. 15, 2014
Shear Test Concept Design	5	Oct. 6, 2014	Oct. 15, 2014	5 Oct. 6, 2014 Oct. 15, 2014
Structural Concept Design	5	Oct. 6, 2014	Oct. 15, 2014	5 Oct. 6, 2014 Oct. 15, 2014
Design Review 1	1	Sep. 29, 2014	Oct. 15, 2014	1 Sep. 29, 2014 Oct. 15, 2014
Initial Concept Analysis and Selection	10	Oct. 16, 2014	Oct. 21, 2014	5 Oct. 16, 2014 Oct. 21, 2014
Dimension Design	2	Oct. 22, 2014	Oct. 22, 2014	2 Oct. 22, 2014 Oct. 31, 2014
Engineering Analysis	10	Oct. 23, 2014	Oct. 28, 2014	10 Oct. 22, 2014 Oct. 28, 2014
Actuator/Sensor Estimated Specs	1	Oct. 28, 2014	Oct. 29, 2014	1 Oct. 28, 2014 Nov. 5, 2014
Phase 1 Report	4	Oct. 15, 2014	Oct. 29, 2014	6 Oct. 15, 2014 Nov. 5, 2014
Refinement/Iteration of Design	5	Oct. 30, 2014	Nov. 3, 2014	80 Oct. 30, 2014 Feb. 28, 2015
CAD Modelling	10	Nov. 3, 2014	Nov. 12, 2014	25 Nov. 3, 2014 Feb. 28, 2015
Design Review 2	1	Oct. 29, 2014	Nov. 12, 2014	1 Nov. 5, 2014 Nov. 12, 2014
FEA Analysis	10	Nov. 12, 2014	Nov. 21, 2014	10 Nov. 12, 2014 Feb. 28, 2015
Material Selection	2	Nov. 21, 2014	Nov. 23, 2014	5 Nov. 21, 2014 Feb. 2, 2015
Oral Presentation	2	Nov. 12, 2014	Nov. 26, 2014	2 Nov. 12, 2014 Nov. 26, 2014
Phase 2 Report	10	Nov. 26, 2014	Dec. 3, 2014	10 Nov. 26, 2014 Dec. 5, 2014
Actuator/Sensor Final Specs/Selection	5	Dec. 3, 2014	Dec. 7, 2014	50 Dec. 3, 2014 Feb. 13, 2015
Initial Prototype	20	Dec. 7, 2014	Jan. 9, 2015	60 Feb. 28, 2015 Mar. 9, 2015
Interface Coding	15	Dec. 7, 2014	Jan. 9, 2015	10 Feb. 28, 2015 Mar. 25, 2015
Prototype Testing Phase 1	15	Jan. 9, 2015	Jan. 18, 2015	10 Jan. 9, 2015 Mar. 25, 2015
Design Analysis Report	10	Dec. 3, 2014	Jan. 21, 2015	10 Dec. 5, 2014 Feb. 2, 2015
Prototype Iteration	20	Jan. 21, 2015	Feb. 1, 2015	20 Mar. 25, 2015 Apr. 8, 2015
Prototype Testing Phase 2	15	Feb. 2, 2015	Feb. 13, 2015	0 N/A N/A
Detailed Design Documentation	10	Jan. 21, 2015	Feb. 13, 2015	10 Feb. 2, 2015 Mar. 9, 2015
Prototype Iteration	20	Feb. 14, 2015	Mar. 4, 2015	0 N/A N/A
Physical Prototype Demonstration	1	Feb. 13, 2015	Mar. 4, 2015	0 N/A N/A
Final Prototype	10	Mar. 5, 2015	Mar. 25, 2015	0 N/A N/A
Testing and Validation Report	10	Mar. 4, 2015	Mar. 18, 2015	0 N/A N/A
Showcase Presentation	3	Mar. 18, 2015	Mar. 25, 2015	10 Mar. 18, 2015 Mar. 25, 2015
Final Report	10	Mar. 25, 2015	Apr. 8, 2015	10 Mar. 25, 2015 Apr. 8, 2015
Reflections and Lessons Learned	4	Mar. 25, 2015	Apr. 8, 2015	4 Apr. 4, 2015 Apr. 8, 2015
Total	271		385	

## **Conclusion**

The purpose of this design project was to test and verify a method of estimating planetary terrain parameters using a simplified rocker bogie model that was developed by David Michel. To accomplish this, a micro-bevameter was fully designed and an initial prototype was developed. This prototype conducts all of the required movements for both the pressure-sinkage and shear-slippage tests necessary. However, due to a number of setbacks, the sensors have yet to be fully calibrated and installed, and thus the algorithm developed by David Michel has not been presently verified.

## **Recommendations**

In order to move forward with the project, all of the suggested modifications described in the modifications and improvements section above should be implemented. These included obtaining a power supply for the prototype, a micro-SD card for data collection, the installation of both the strain gauges, the load cell and the linear bearing, and the design and implementation of a device to accurately measure the degree of the base plate. Once this is done, the onboard sensors should be re-calibrated, and then the full testing phase of this project can continue. The next step is to test the output data of this prototype with a soil with known parameters to verify the accuracy of the bevameter.

In addition to the bevameter, the onboard sensors of the LunaTron Rover need to be calibrated in order to test the algorithm developed by David Michel. Once this is done, the bevameter and the rover can be taken out for field testing.

## References

- 1 Michel, David. System of Terrain Analysis, Energy Estimation and Path Planning for Planetary Exploration by Robot Teams. London, Ontario, Canada: University of Western Ontario, 2012. Thesis.
- 2 Cross, Matthew. Estimating Terrain Parameters With a Rigid Wheeled Rover Using Neural Networks. Ottawa, Ontario, Canada: Carleton U, 2012. Thesis.
- 3 Golob, T. B. *Soil Strength Instrumentation and Methodology of Measurements*. Chalk River, Ont.: Petawawa National Forestry Institute, 1982. Print.
- 4 Wong, J. Y. Terramechanics and Off-road Vehicle Engineering Terrain Behaviour, Off-road Vehicle Performance and Design. 2nd ed. Amsterdam: Elsevier, 2010. Print.
- 5 Murphy, Michelle. "New Lunar Tool Invented at Glenn." NASA. NASA, 1 Jan. 2010. Web. 5 Nov. 2014.  
<[http://www.nasa.gov/centers/glenn/multimedia/imagegallery/if\\_59\\_vacuum.html#.VFmdPsm6gV4](http://www.nasa.gov/centers/glenn/multimedia/imagegallery/if_59_vacuum.html#.VFmdPsm6gV4)>
- 6 Hoffman, Karl. "Applying the Wheatstone Bridge Circuit". Hottinger Baldwin Messtechnik GmbH, Web Apr. 8, 2015,. <<http://www.hbm.com.pl/pdf/w1569.pdf>>

## Appendix I – Strain Gauge Formation as a Wheatstone Bridge

Foil strain gauges will be used in a Wheatstone bridge configuration to read the torque on the shaft. These will be placed above the base plate to accommodate for torque losses in the system.

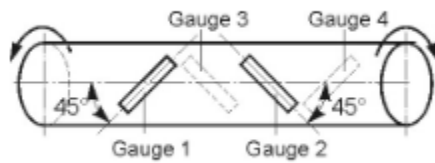


Figure 22: Strain gauge layout on shaft [6].

The circuit layout is as follows:

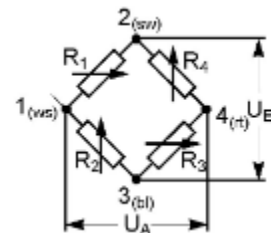


Figure 23: Strain gauge circuit layout [6].

## Appendix II – Initial Gantt Chart

Task Name	Q3			Q4			Q1			Q2		
	Jul	Aug	Sep	Oct	Nov	Dec	Jan	Feb	Mar	Apr	May	Jun
1 Project Proposal												
2 Terramechanics Research												
3 Calibrate Existing Rover Sensors												
4 Pressure/Sinkage Device Design												
5 Shear Test Device Design												
6 Rover Mount Design												
7 Design Review 1												
8 Concept Analysis and Selection												
9 Dimension Design												
10 Engineering Analysis												
11 Actuator/Sensor Estimated Specs												
12 Phase 1 Report												
13 Refinement/Iteration of Design												
14 CAD Modelling												
15 Design Review 2												
16 FEA Analysis												
17 Material Selection												
18 Oral Presentation												
19 Actuator/Sensor Final Specs												
20 Phase 2 Report												
21 Initial Prototype												
22 Interface Coding												
23 Prototype Testing Phase 1												
24 Design Analysis Report												
25 Prototype Iteration												
26 Prototype Testing Phase 2												
27 Detailed Design Documentation												
28 Prototype Iteration												
29 Physical Prototype Demonstration												
30 Final Prototype												
31 Testing and Validation Report												
32 Showcase Presentation												
33 Final Report												
34 Reflections and Lessons Learned												

### Appendix III - Shaft Selection Analysis

There are four different shaft types available on McMaster-Carr [1], given as:

Table 6: Available shaft materials and the respective costs for 3 ft. with a 3/4" diameter

Shaft Material	Cost for 3/4", 3 ft. Shaft (\$)
1045 Steel Shaft	42.88
304 Stainless Steel	114.98
316 Stainless Steel	160.32
2024-T4 Aluminum <sup>◊</sup>	47.40

◊ - only available in 2 ft.

During the pressure-sinkage and shear-slipage tests, the shaft of the bevameter may undergo a compression force of up to 80 N and torque of up to 4.8 Nm. The shaft must be able to withstand these loads without buckling or deflecting laterally or angularly in any significant way. First, the critical buckling load of the shaft was determined. The critical load can be determined using either the Euler or Johnson formulas, depending on the type of shaft used [1]. To classify the bevameter shaft, the slenderness ratio will be used:

$$S = \frac{L_e}{r}$$

Where  $L_e = CL$  is the effective length of the rod and  $r = \sqrt{\frac{I}{A}}$  is the radius of gyration. The effective length constant C can be determined based on the columns boundary conditions (fixed – guided, thus  $C = 1$  [Error! Bookmark not defined.]). The moment of inertia I for a solid cylinder is [1]:

$$I = \frac{\pi r^4}{4}$$

Therefore the Slenderness Ratio can be found to be:

$$S = \frac{2CL}{r}$$

Given the shaft length  $L = 350.79$  mm and the shaft radius  $r = 9.53$  mm, the Slenderness Ratio is found to be  $S = 73.7$ .

If the slenderness ratio is greater than the critical slenderness ratio, then the Euler formula is used and the shaft is considered a long column. Otherwise, the Johnson formula is applied [Error! Bookmark not defined.]. The critical slenderness ratio is given as:

$$S_{cr} = \sqrt{\frac{2\pi^2 E}{\sigma_y}}$$

Using the cheapest available shaft material of 1045 carbon steel, rolled, with a Young's Modulus of  $E = 212.4$  GPa and a Yield Strength of  $\sigma_y = 417.1$  MPa, the Critical Slenderness Ratio was found to be  $S_{cr} = 100.3$ .

Since  $S < S_{cr}$ , while under a load this shaft is considered to be a short column, and therefore to calculate the critical buckling load the Johnson formula must be used. With an expected maximum torque of 4.8 Nm applied to the shaft, the critical buckling load is [Error! Bookmark not defined.]:

$$P_{cr} = \sigma_y A \left[ 1 - \frac{\sigma_y}{4\pi^2 E} \left( \frac{L_e}{r} \right)^2 \right] - \frac{T^2}{E\pi r^4} = 110.85 \text{ KN}$$

Since  $P_{cr} \gg F_{max}$ , where  $F_{max}$  is the maximum force that will be applied during the pressure-sinkage test of 80N (which is negligible when compared to the critical buckling load), the buckling of the shaft doesn't need to be considered during the material selection design process, and the yield strength of the material should not be a significant factor for the final material choice.

Instead, the focus will be shifted towards minimizing the elastic deflection of the shaft caused by the applied torque from the motor and the resulting reaction between the base plate (attached to the shaft) and the ground. This equation is given by **[Error! Bookmark not defined.]**:

$$\theta = \frac{LT}{KG}$$

With the shaft length L, moment K, and maximum expected torque T all known, the only material property that can affect the elastic deflection is the shear modulus G. By maximizing G, the angular deflection of the shaft can be minimized.

The second main parameter to consider is the Young's modulus of the material. By maximizing the rigidity of the shaft as well, the elastic deformation of the shaft will decrease, making it less likely that the shaft will bend and seize up with other components of the design. With these two mechanical properties in mind, the following plot was created using CES for the available shaft materials:

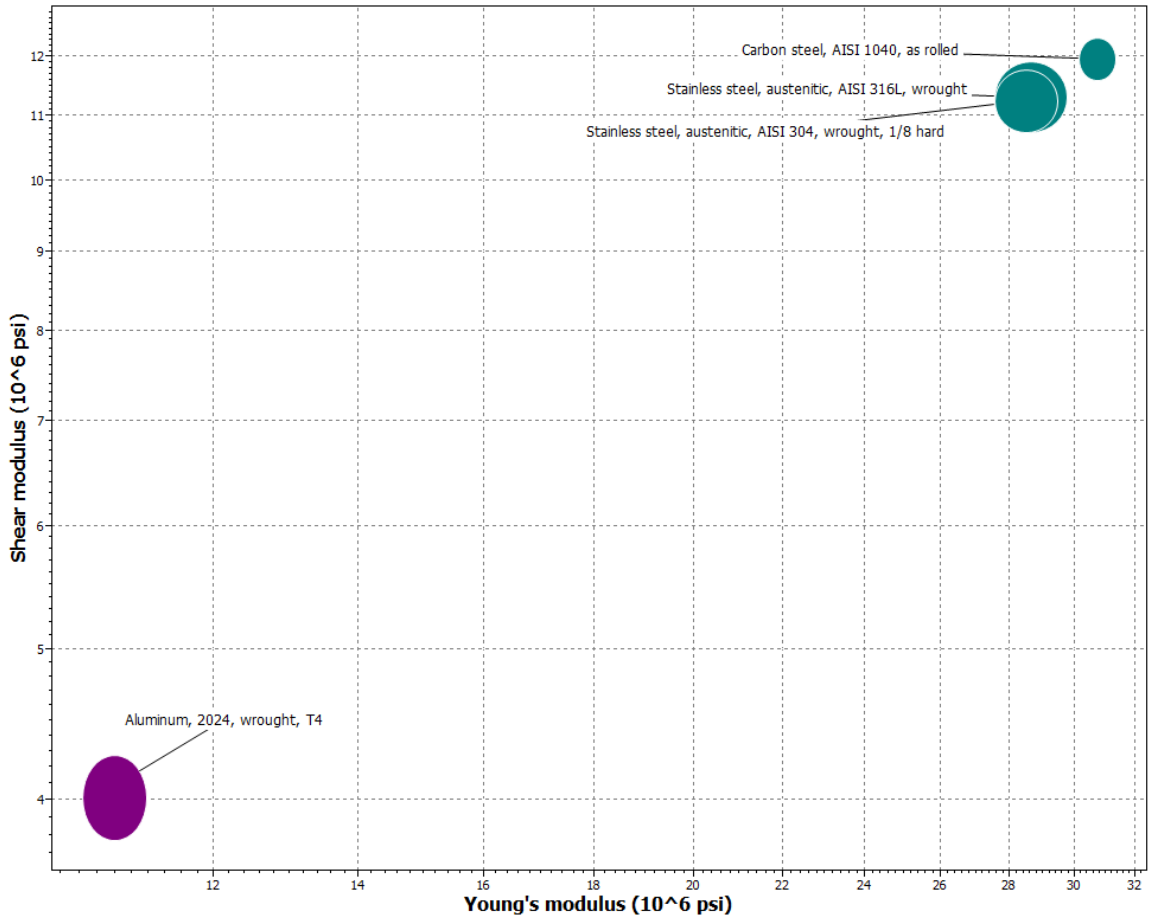


Figure 24: CES of Shear Modulus and Young's Modulus of potential shaft materials

From this plot it is obvious that the aluminum shaft is the worst candidate for the bevameter. Of the three remaining materials, carbon steel was chosen as the final shaft material. It has the highest shear and Young's modulus, and is the cheapest of the three remaining options, making it both the best and the only feasible option available.

## Appendix IV - Frame Material Analysis

The structural frame of the bevameter will be made of rectangular framing tubes. There is a wide selection of materials available to choose from on McMaster-Carr for this component [Error! Bookmark not defined.]. These were all taken and compared with respect to their cost and their rigidity to find the most suitable material for this application. This can be seen in the plot below:

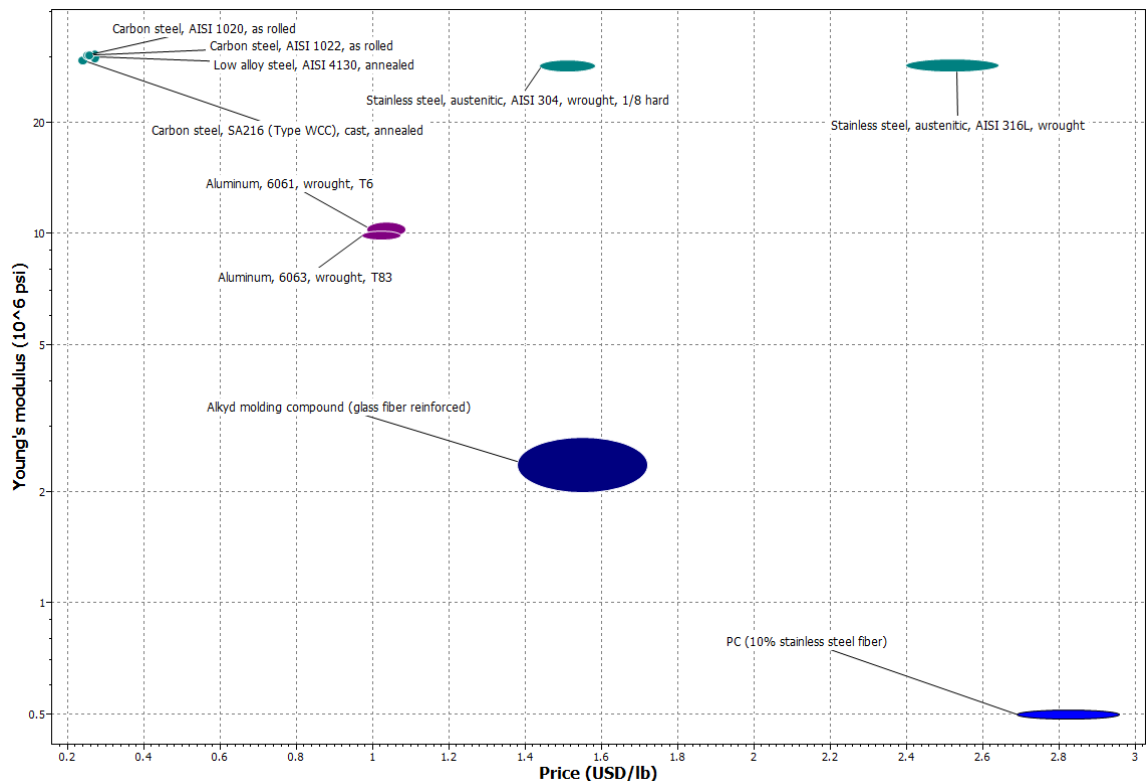


Figure 25: CES of Young's Modulus and Cost of potential structural framing materials.

The materials of interest appear in the upper left section of the plot, having the highest Young's modulus and the lowest cost. 1020 carbon steel rectangular tubing was then selected for the bevameter design

## **Appendix V – PCB Components**

These are the components necessary to complete the PCB design included in this report:

Table 7: Components required for the PCB

Resistor, SM 1206	4 x 100 ohm
	1 x 3k ohm
	3 x 1k ohm
LT 1167	3
Capacitor, SM 1206	3 x 1uF
Female headers (0.100" pitch)	2 x 2 pin
	1 x 3 pin
	2 x 4 pin
	1 x 5 pin
	1 x 6 pin
Male headers (0.100" pitch)	1 x 6 pin
	2 x 8 pin
	1 x 10 pin
6mm tact switch (button)	1

A UBEC is also needed, to convert from 12V to 3.3V. Consider using the X3 PRO 3.3V 3.5A UBEC, although a better alternative may be found.

## Appendix VI – Base Plate Size Script

```
%This script estimates the sizes of the baseplates we'll need for multiple
%normal forces and wheel sizes by estimating the depth to which the
%baseplate will go based on terrain parameter estimations (Wong, 2010), and
%then by calculating the angle of contact of the wheel. This angle is used
%to find the contact area of the wheel to the ground, and then a baseplate
%radius that corresponds to this area is found.

close all
clear
clc

F1 = 80;
F2 = 20;

% radii and wheel width are equal
r = [5,7.5,10];

%LETE Sand
n1 = 0.611; % soil deformation exponent
kphi1 = 475; %soil modulus of friction
kc1 = 1.16; %soil modulus of cohesion
%Sandy Loam
n2 = 0.850; % soil deformation exponent
kphi2 = 2529; %soil modulus of friction
kc2 = 3.3; %soil modulus of cohesion
%Clayey Loam
n3 = 0.850; % soil deformation exponent
kphi3 = 1131; %soil modulus of friction
kc3 = 6.8; %soil modulus of cohesion

for i = 1:1:3
%estimated terrain depth
z1(i) = ((3*F1)/(r(i)*((2*r(i))^0.5)*(3-n1)*(kphi1+kc1/r(i))))^(2/(2*n1+1));
z2(i) = ((3*F1)/(r(i)*((2*r(i))^0.5)*(3-n2)*(kphi2+kc2/r(i))))^(2/(2*n2+1));
z3(i) = ((3*F1)/(r(i)*((2*r(i))^0.5)*(3-n3)*(kphi3+kc3/r(i))))^(2/(2*n3+1));
%Resulting angle of contact
thetaC1(i) = acosd(1-z1(i)/r(i));
thetaC2(i) = acosd(1-z2(i)/r(i));
thetaC3(i) = acosd(1-z3(i)/r(i));
%Contact area
A1(i) = r(i)^2 * thetaC1(i);
A2(i) = r(i)^2 * thetaC2(i);
A3(i) = r(i)^2 * thetaC3(i);
%Baseplate radii
rf1(i) = sqrt(A1(i)/pi);
rf2(i) = sqrt(A2(i)/pi);
rf3(i) = sqrt(A3(i)/pi);
R(i,:) = [rf1(i),rf2(i),rf3(i)];
end;
Wheel0R = R(1,:);
Wheel1R = R(2,:);
Wheel2R = R(3,:);
```

## Appendix VII – MATLAB Parameter Calculation Script

### Main Script

```
clc
clear

%///////////
%DATA IMPORTING CODE HERE
%3 Tests per baseplate, b# = baseplate number, t# =
experiment number
%Should have 3 vectors of force readings and 3 of sinkage
readings per
%plate, as well as an overall size of each vector pair

%///////////

b1 = 0.057; %Base plate radii meters
b2 = 0.066;

%///////////
%Force to pressure conversion
%All 3 force vectors for each baseplate test will be
converted to pressures
%by dividing them by their respective base plate surface
areas

%Pi = Pressure( Fi, sizei, bi )
%///////////
InterpSize = 100; %Doesn't change interpolate or average
functions!
%Calculate the average (best fit curve) of the data
Zavg1 = Average(P11, P12, P13, Z11, Z12, Z13);
Zavg2 = Average(P21, P22, P23, Z21, Z22, Z23);
Pavg = 0:100:7800; %Interpolation size...
%Calculate Beckers Parameters
[ navg, Kphi, Kc ] = calculateParameters( Pavg, Zavg1,
Zavg2, InterpSize, B1, B2 );
%Pressure Sinkage Parameters Have Been Calculated!!!
navg
Kphi
Kc

%SHEAR SLIPPAGE
```

```

k = 0; %Gage Factor
UE = 5; %Input Voltage
%Two arrays, UA1, UA2, for voltage changes in strain gages
%Two arrays, j1 and j2 for angular position
%Two values, UA1Size, UA2Size
%Two pressures, PA1, PA2, for pressures test was conducted
under
G = 0; %Shear factor for steel shaft

%Convert UA arrays into shear arrays
[s1, s1max] = shearConversion( G, UE, K, UA1, UA1Size);
[s2, s2max] = shearConversion( G, UE, K, UA2, UA2Size);

%Calculate c and phi
%smax = c + P*tan(phi)
phi = atand((s1max - s2max)/(PA1 - PA2));
c = s1max - PA1*tan(phi);%cohesion

%Calculate K
%First plot and display s1/s1max by j displacement plot

%Next ask user what the plot looks like
prompt = 'Is the curve exponential(1),\ndoing it peak and
then continually decrease(2), \nor does it peak and then
level out(3)?\n';
x = input(prompt);
if x == 1
    K = calculateKExp( s1, UA1Size, s1max, j1 );
end
if x == 2
    y = calculateKPeakDown( s1, UA1Size, s1max, j1 );
end
if x == 3
    %y = ...
end

```

### **Pressure Conversion Function**

```

function [ P ] = Pressure( F, size, b )
%Solve Pressure Array
%    Take Force value and divide by baseplate size

for i = 1:1:size
    P(i) = F(i) / (3.1415*b^2);

```

```

end
end
```

### **Average Pressure Calculation Function**

```

function [ Zavg ] = Average( P1, P2, P3, z1, z2, z3 )
%Average
% Finds the average of the three test values using
% interpolated data sets
z1I = Interpolate(P1,z1);
z2I = Interpolate(P2,z2);
z3I = Interpolate(P3,z3);
for i = 1:100          %Interp Size!
    Zavg(i) = (z1I(i) + z2I(i) + z3I(i))/3;
end
end
```

### **Interpolation Function**

```

function [ zf ] = Interpolate( P, zi )
%Interpolate data points for pressure-sinkage curve
% from 0 - 80N
Pavg = 0:100:7800; %array of points from 0 to 7838 N/m^2
pressure (80N force)
zf = interp1(P,zi,Pavg, 'spline'); %interpolate
end
```

### **Pressure-Sinkage Parameter Calculation Function**

```

function [ navg, Kphi, Kc ] = calculateParameters( Pavgl,
Zavgl, Zavg2, Size1, b1, b2 )
%Calculate three beckers parameters
navg = calculateNAvg( Pavgl, Zavgl, Zavg2, Size1 );

[ p2, p2lnp, p2lnz, p2lnz2, p2lnzlnp ] = Summations( Pavgl,
Zavgl, Size1 );
Keq1 = exp((p2lnp - navg*p2lnz)/p2);

[ p2, p2lnp, p2lnz, p2lnz2, p2lnzlnp ] = Summations( Pavgl,
Zavg2, Size1 );
Keq2 = exp((p2lnp - navg*p2lnz)/p2);

Kc = (Keq1-Keq2) * (b2*b1) / (b2-b1)
```

```

Kphi = -(Keq1-Keq2)*(b2)/(b2-b1)
end

```

### ***N<sub>avg</sub>* Calculation Function**

```

function [ navg ] = calculateNAvg( Pavg, Zavg1, Zavg2,
Size1 )
% Calculate parameter navg

[ p2, p2lnp, p2lnz, p2lnz2, p2lnzlnp ] = Summations( Pavg,
Zavg1, Size1 );
n1 = (p2*p2lnzlnp-p2lnz*p2lnp)/(p2*p2lnz2-p2lnz^2);

[ p2, p2lnp, p2lnz, p2lnz2, p2lnzlnp ] = Summations( Pavg,
Zavg2, Size1 );
n2 = (p2*p2lnzlnp-p2lnz*p2lnp)/(p2*p2lnz2-p2lnz^2);

navg = (n1 + n2)/2;
end

```

### ***Summations Function***

```

function [ p2, p2lnp, p2lnz, p2lnz2, p2lnzlnp ] =
Summations( Pavg, Zavg, size1 )
%Summations
% Calculates the five summations needed for the parameter
equations
p2 = 0;
p2lnp = 0;
p2lnz = 0;
p2lnz2 = 0;
p2lnzlnp = 0;
for i = 1:size1
    p2 = Pavg(i).^2 + p2;
end
for i = 1:size1
    p2lnp = (Pavg(i)^2)*log(Pavg(i)) + p2lnp;
end
for i = 1:size1
    p2lnz = (Pavg(i)^2)*log(Zavg(i)) + p2lnz;
end
for i = 1:size1
    p2lnz2 = (Pavg(i)^2)*(log(Zavg(i)))^2 + p2lnz2;
end
for i = 1:size1

```

```

    p2lnzlnp = (Pavg(i)^2)*log(Zavg(i))*log(Pavg(i)) +
p2lnzlnp;
end
end

```

### ***Shear Conversion Function***

```

function [ s, smax ] = shearConversion( G, UE, K, UA,
UASize)
%Convert wheatstone bridge voltage readings into shear
values
smax = 0;
for i = 1:1:UASize
    Epsilon = UA(i)/(K*UE);
    s(i) = G*Epsilon;
    if(smax < s(i))
        smax = s(i);
    end
end
end

```

### ***CalculateKExp Function (Exponential output curve)***

```

function [ Kexp ] = calculateKExp( S, SSize, smax, j )
%If curve shows exponential form
%Assuming j is the angular position in degrees?

sumNum = 0;
sumDen = 0;

for i = 1:SSize
    sumNum = ((1-S(i)/smax)^2)*j(i)^2 + sumNum;
end

for i = 1:SSize
    sumDen = ((1-S(i)/smax)^2)*j(i)*(log(1-S(i)/smax)) +
sumDen;
end

Kexp = -sumNum/sumDen;
end

```

**CalculateKPeakDown Function (Output curve that peaks then drops)**

```
function [ K ] = calculateKPeakDown( S, SSize, smax, j )
%If curve shows exponential form
%Assuming j is the angular position in degrees?
syms Kw
r = 0;
for i = 1:1:SSize
    r = r + ((S(i)/smax)^2)*(log(S(i)/smax)-(1 +
log(j(i)/Kw)-(j(i)/Kw)))*(Kw - j(i));
end
r
K = solve(r, 0);
```

## Appendix VIII – Run Code

```
*****
LunaTron Terramechanics Terrain Sensor (LT3S)
Code for the micro-bevameter designed for use with the micro-
rover LunaTron at Western University.
(c) Nicole Devos, March 2015

List of updates:
April 2015, Nicoe Devos
***** */

//you might need this library:
//#include <SPI.h>
#include "SD.h"

const int LPWMPin = 11;
const int GPWMPin = 5;
const int LDirPin = 13;
const int GDirPin = 0;
const int LAPos = A0;
const int GEnc1 = 2;
const int GEnc2 = 3;
const int strain1 = A1;
const int strain2 = A2;
const int forcePin = A3;
const int button = 8;

bool enable = LOW;
int pressure = 0;
int shear = 0;

//pre-calibration values, use calib.ino to find these values
//prior to running this code
const float fScale = 1;
const float fOffset = 0;
const float s1Scale = 1;
const float s2Scale = 1;
const float s10Offset = 0;
const float s20Offset = 0;
const float lScale = 1;

//this value will change when the bevameter self-calibrates
float lOffset = 0;

int testDist = 5;
int testAngle = 5;
int testForce1 = 20;
int testForce2 = 40;
int maxForce = 80;
int maxAngle = 180;

//change these as needed (PWM value for L and G motors)
const int maxL = 40;
```

```

const int maxG = 35

const int pollCount = 5;
float forceAvg = 0;
float force[pollCount] = {0};
float strainAvg[2] = {0};
float strain[2][pollCount] = {0};
float distAvg = 0;
float dist[pollCount] = {0};

void setup()
{
    //initialize pins
    pinMode(LPWMPin, OUTPUT);
    pinMode(LDirPin, OUTPUT);
    pinMode(GPWMPin, OUTPUT);
    pinMode(GDirPin, OUTPUT);
    pinMode(LAPos, INPUT);
    pinMode(GEnc1, INPUT);
    pinMode(GEnc2, INPUT);
    pinMode(strain1, INPUT);
    pinMode(strain2, INPUT);
    pinMode(forcePin, INPUT);

    //set up internal pullup resistors
    digitalWrite(LAPos, HIGH);
    digitalWrite(strain1, HIGH);
    digitalWrite(strain2, HIGH);
    digitalWrite(forcePin, HIGH);

    //setup external interrupts for digital encoder
    attachInterrupt(GEnc1, encoder1, RISING);
    attachInterrupt(GEnc2, encoder2, RISING);

    //setup SD card
    SD.begin();

    //for debugging, uncomment these lines:
    //Serial.begin(9600);
}

void loop()
{
    //run code, comment this section out to debug
    if (button)
    {
        if (pressure < 2)
            pressureTest
        else
            shearTest
    }

    //uncomment this section for debugging, comment out
    //previous section
    ****
}

```

```

checkSerial();
if (enable)
{
  if ((analogRead(LAPos) < 200) && (state == 0))
  {
    digitalWrite(LDirPin, HIGH);
    analogWrite(LPWMPin, 40);
  }
  else if (state < 1)
  {
    analogWrite(LPWMPin, 0);
    state = 1;
  }
  if ((analogRead(LAPos) >= 200) && (state == 1))
  {
    analogWrite(GPWMPin, 35);
    delay(2000);
    analogWrite(GPWMPin, 0);
    state = 2;
  }
  if ((analogRead(LAPos) > 63) && (state == 2))
  {
    digitalWrite(LDirPin, LOW);
    analogWrite(LPWMPin, 40);
    if (analogRead(LAPos) < 63)
    {
      enable = 0;
    }
  }
}
*****/
}

//Pressure-Sinkage test
void pressureTest()
{
  calibrate();
  while(forceAvg < maxForce)
  {
    while(distAvg < testDist)
    {
      lDown();
      distCalc();
    }
    stopMotor();
    forceCalc();
    writeSD();
    testDist++;
  }
  pressure++;
  shear = 0;
  lUp();
}

//Shear-Slippage test
void shearTest()

```

```

{
    calibrate();
    if(shear == 0)
    {
        int testForce = testForce1;
    }
    else
    {
        int testForce = testForce2;
    }
    while(forceAvg < testForce)
    {
        lDown();
        forceCalc();
    }
    stopMotor();
    while(testAngle < maxAngle)
    {
        while(angleAvg < testAngle)
        {
            cTurn();
            angleCalc();
        }
        stopMotor();
        forceCalc();
        strainCalc();
        writeSD();
        testAngle += 5;
    }
    shear++;
    lUp();
    ccTurn();
    if (shear == 2)
    {
        pressure = 0;
    }
}

void calibrate()
{
    lUp();
    while(forceAvg <= 0)
    {
        forceCalc();
    }
    lOffset = distAvg;
    lUp();
}

void lUp()
{
    while(analogRead(LAPos) > 63)
    {
        digitalWrite(LDirPin, LOW);
        analogWrite(LPWMPin, maxL);
    }
}

```

```

}

void lDown()
{
    digitalWrite(LDirPin, HIGH);
    analogWrite(LPWMPin, maxL);
}

void cTurn()
{
    digitalWrite(GDirPin, HIGH);
    analogWrite(GPWMPin, maxG);
}

void ccTurn()
{
    cli();
    while(encoder1 > 0)
    {
        digitalWrite(GDirPin, LOW);
        analogWrite(GPWMPin, maxG);
    }
    stopMotor();
    sei();
}

void stopMotor()
{
    analogWrite(LPWMPin, 0);
    analogWrite(GPWMPin, 0);
}

void forceCalc()
{
    forceAvg = 0;
    for (int n = 1; n < pollCount; n++)
    {
        forceAvg += (force[n-1] = force[n]);
    }
    forceAvg += (force[pollCount-1] = readForce());
    forceAvg /= pollCount;
}

float readForce()
{
    return ((fScale * analogRead(forcePin)) - fOffset);
}

void strainCalc()
{
    for (i = 0; i < 2; i++)
    {
        strainAvg[i] = 0;
        for (int n = 1; n < pollCount; n++)
        {
            strainAvg[i] += (strain[i][n-1] = strain[i][n]);
        }
    }
}

```

```

        }
        strainAvg[i] += (strain[i][pollCount-1] = readStrain(i));
        strainAvg[i] /= pollCount;
    }
}

float readStrain(int i)
{
    if(i == 0){
        return ((s1Scale * analogRead(strain1)) - s10ffset);
    }
    else if (i == 1){
        return ((s2Scale * analogRead(strain2)) - s20ffset);
    }
    else
        return 0;
}

void distCalc()
{
    distAvg = 0;
    for (int n = 1; n < pollCount; n++)
    {
        distAvg += (dist[n-1] = dist[n]);
    }
    distAvg += (dist[pollCount-1] = readDist());
    distAvg /= pollCount;
}

float readDist()
{
    return ((lScale * analogRead(LAPos)) - l0ffset);
}

//encoder interrupt codes
void encoder1()
{
    encoder1++;
}

void encoder2()
{
    encoder2++;
}

//write SD
void writeSD()
{
    if (pressure < 2)
    {
        //Open Pressure-Sinkage file
        File pressureSink = SD.open("pressure.txt", FILE_WRITE);

        //Print the distance and force:
        pressureSink.print(pressure);
        pressureSink.print("\t");
    }
}

```

```

pressureSink.print(distAvg);
pressureSink.print("\t");
pressureSink.print(forceAvg);
pressureSink.println();

//Save file and close:
pressureSink.close();
}
else
{
    //Open Shear-Slipage file
    File shearSlip = SD.open("shear.txt", FILE_WRITE);

    //Print the force, angle, and torque
    shearSlip.print(forceAvg);
    shearSlip.print("\t");
    shearSlip.print(angleAvg);
    shearSlip.print("\t");
    shearSlip.print(torqueAvg);
    shearSlip.println();

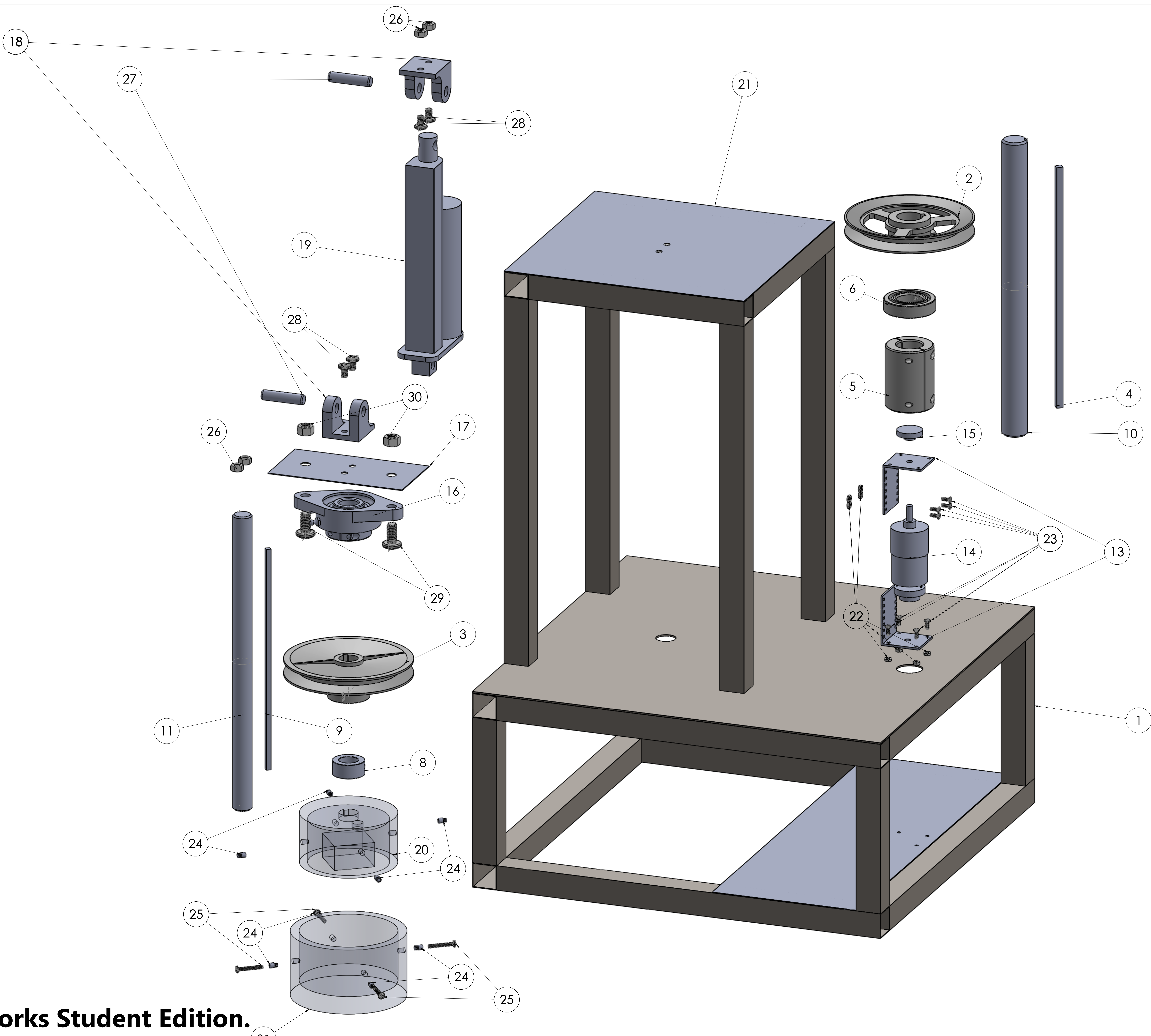
    //Save file and close:
    shearSlip.close();
}
}

//serial commands for debugging
void checkSerial()
{
    if(Serial.available() > 0)
    {
        char input = Serial.read();
        switch (input) {
            case '0':
                enable = !enable;
                if (enable)
                {
                    Serial.println("go");
                    state = 0;
                }
                else
                {
                    Serial.println("no go");
                    digitalWrite(LDirPin, LOW);
                    analogWrite(LPWMPin, 40);
                }
                break;
            case '1':
                Serial.println(analogRead(LAPos));
                break;
            case '2':
                Serial.println(state);
                break;
            //additional cases can be added to test varying
            //functionality
        }
    }
}

```

```
    }  
    else  
        return;  
}
```

## **Appendix IX – Part and Assembly Drawings**

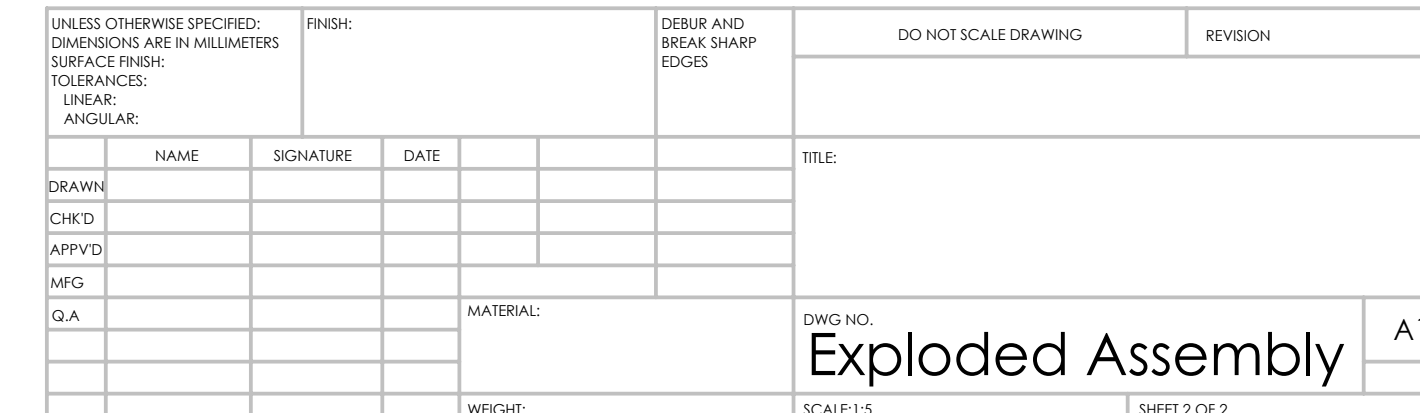


# **SolidWorks Student Edition.**

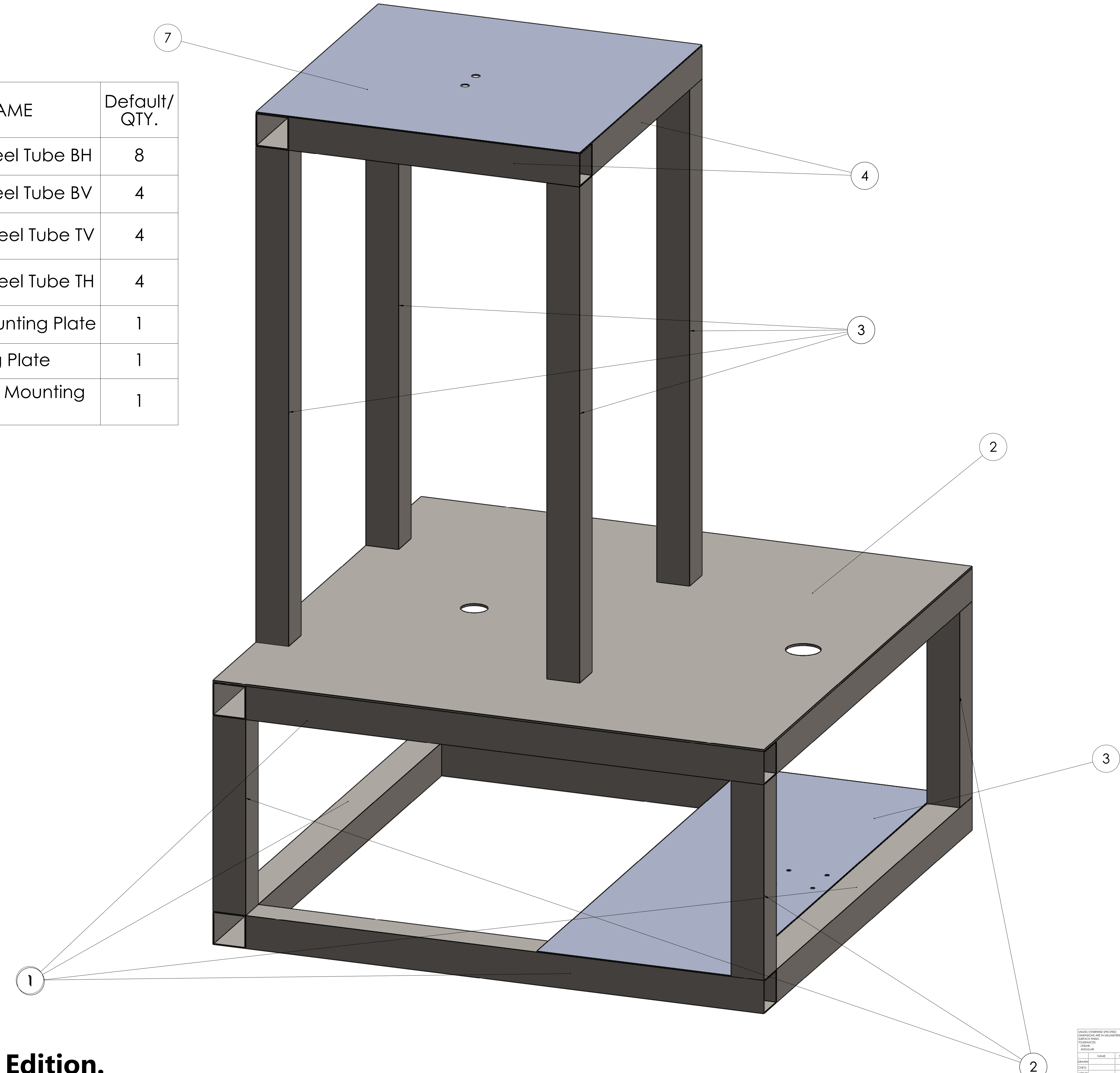
## **For Academic Use Only.**

Part Number	Description	Comment/Notes	Default/QTY.
1	Rectangular Steel Tube		1
2	V-Belt Pulley 5" OD 1" Bore Diameter		1
3	Gearmotor Mounting Plate		2
4	Pulley Mounting Plate		1
5	Rectangular Steel Tube TH		1
6	1" Ball Bearing		1
7	Rectangular Steel Tube TV		2
8	3/4" Set Screw Shaft Collar		2
9	3/16" Keyway Shaft Key		2
10	1" Fully Keyed Shaft		1
11	3/4" Fully Keyed Shaft		2
13	Gearmotor L-Bracket		2
14	Gearmotor		1
15	6mm Gearmotor Mounting Hub		1
16	Mounted Concentric Bearing		1
17	Mounted Concentric Bearing Mounting Plate		1
18	Concentric Linear Actuator Mounting Bracket		2
19	Linear Actuator		1
20	Baseplate Top		1
21	Baseplate Bottom		1
22	5-40 Hex Nut		8
23	5-40 Pan Head Phillips Screw		8
24	Threaded Insert with 6-32 Thread		8
25	6-32 Pan Head Phillips Screw		4
26	1/4"-20 Hex Nut		4
27	6mm Metal Mounting Pin		2
28	1/4"-20 Pan Head Phillips Screw		4
29	3/8"-16 Pan Head Phillips Screw		2
30	3/8"-16 Hex Nut		2

**SolidWorks Student Edition.  
For Academic Use Only.**

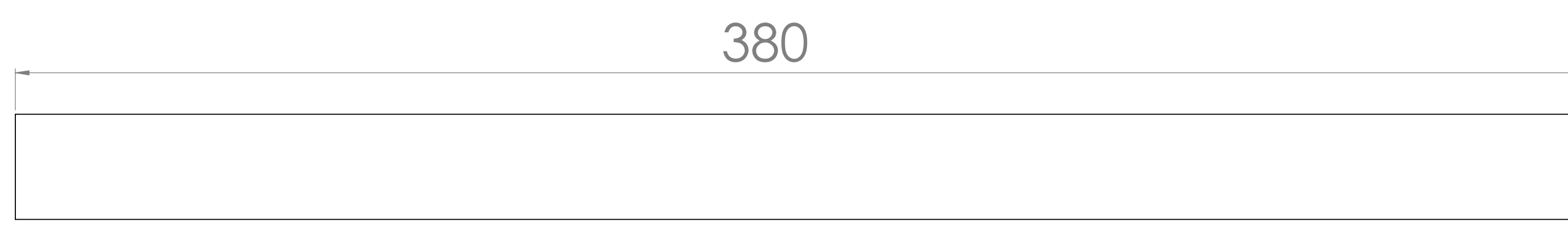


ITEM NO.	PART NAME	Default QTY.
1	Rectangular Steel Tube BH	8
2	Rectangular Steel Tube BV	4
3	Rectangular Steel Tube TV	4
4	Rectangular Steel Tube TH	4
5	Gearmotor Mounting Plate	1
6	Pulley Mounting Plate	1
7	Linear Actuator Mounting Plate	1

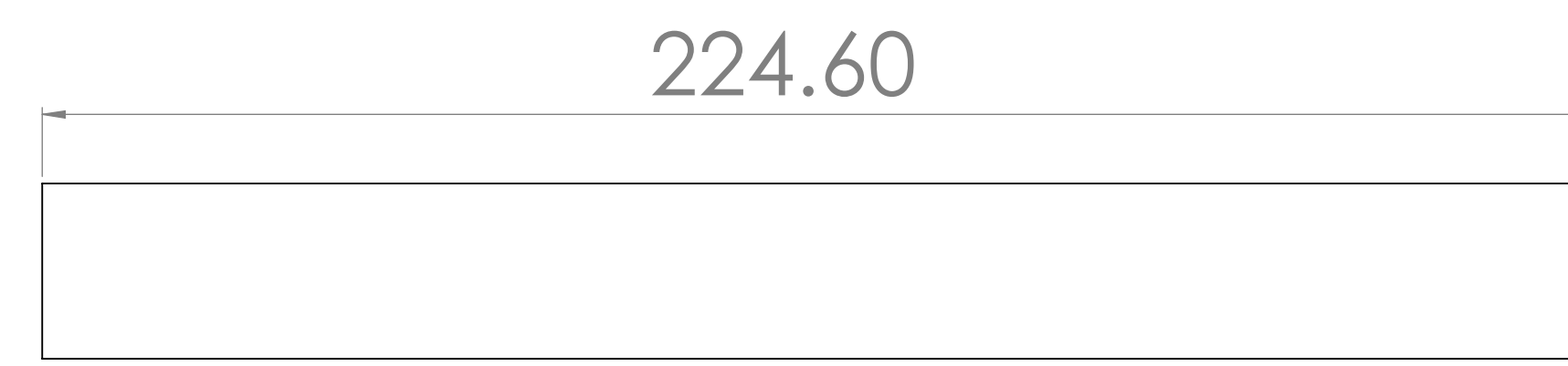


# **SolidWorks Student Edition.**

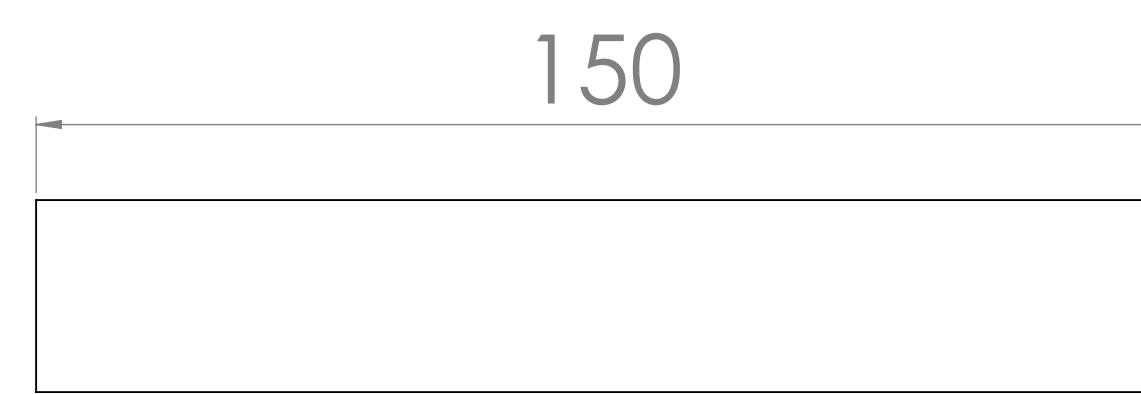
## **For Academic Use Only.**



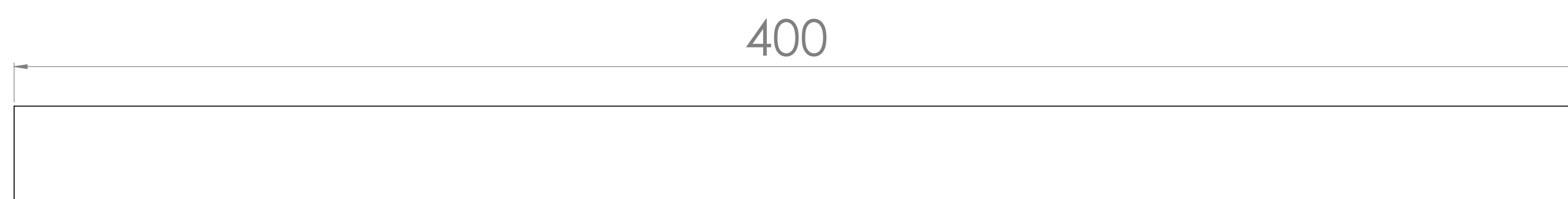
Rectangular Steel Tube TV



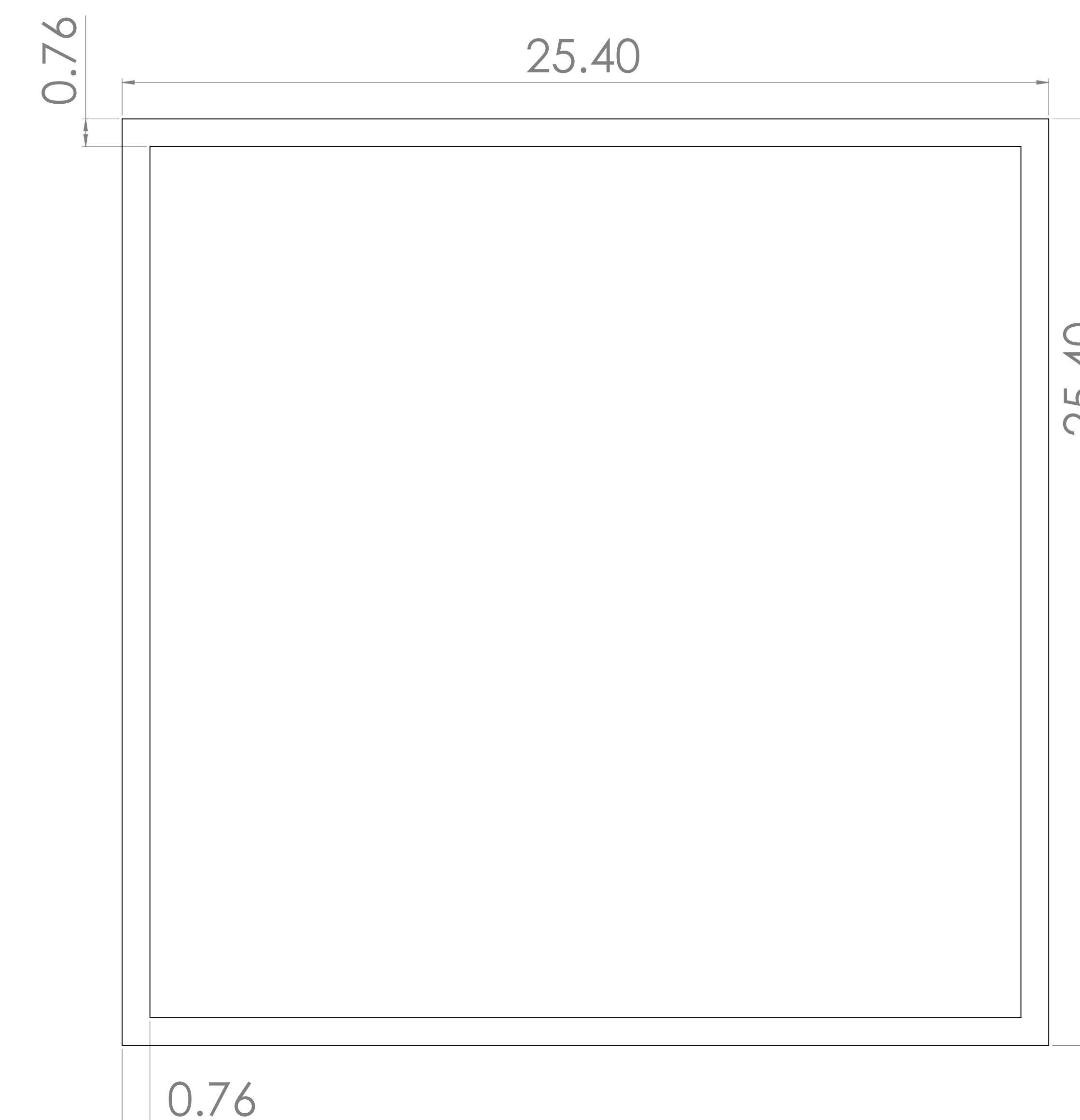
Rectangular Steel Tube TH

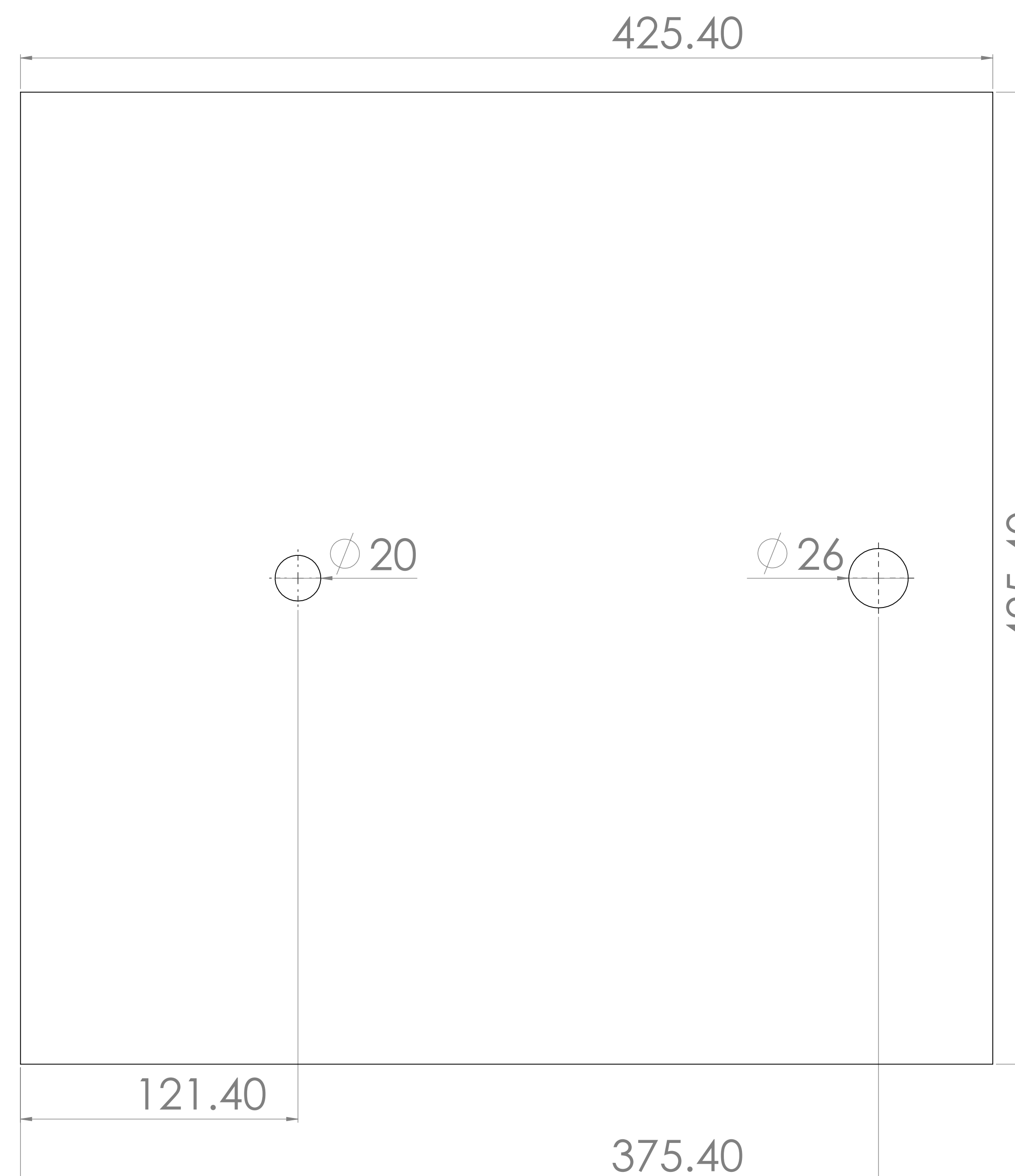


Rectangular Steel Tube BV

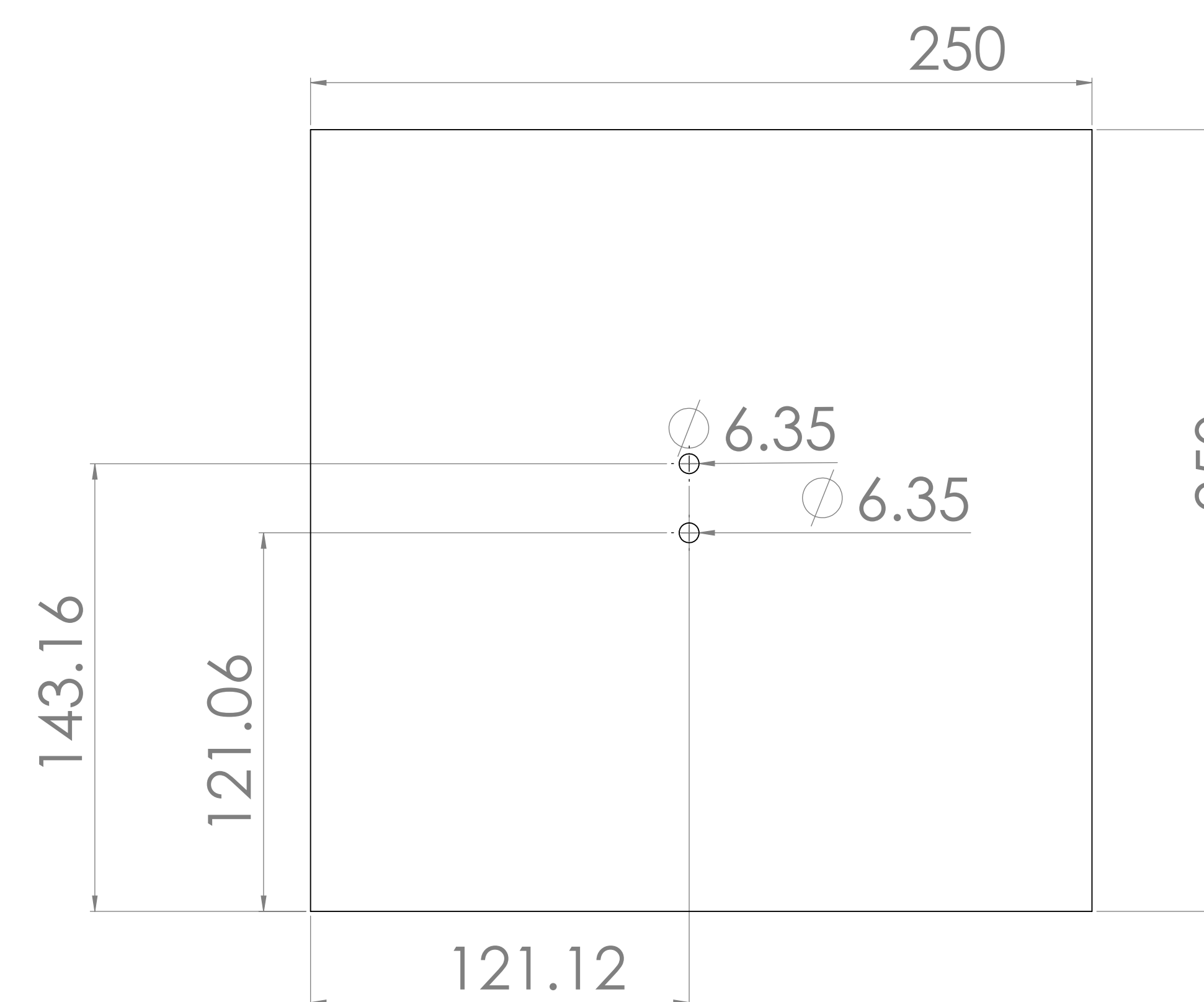


Rectangular Steel Tube BH

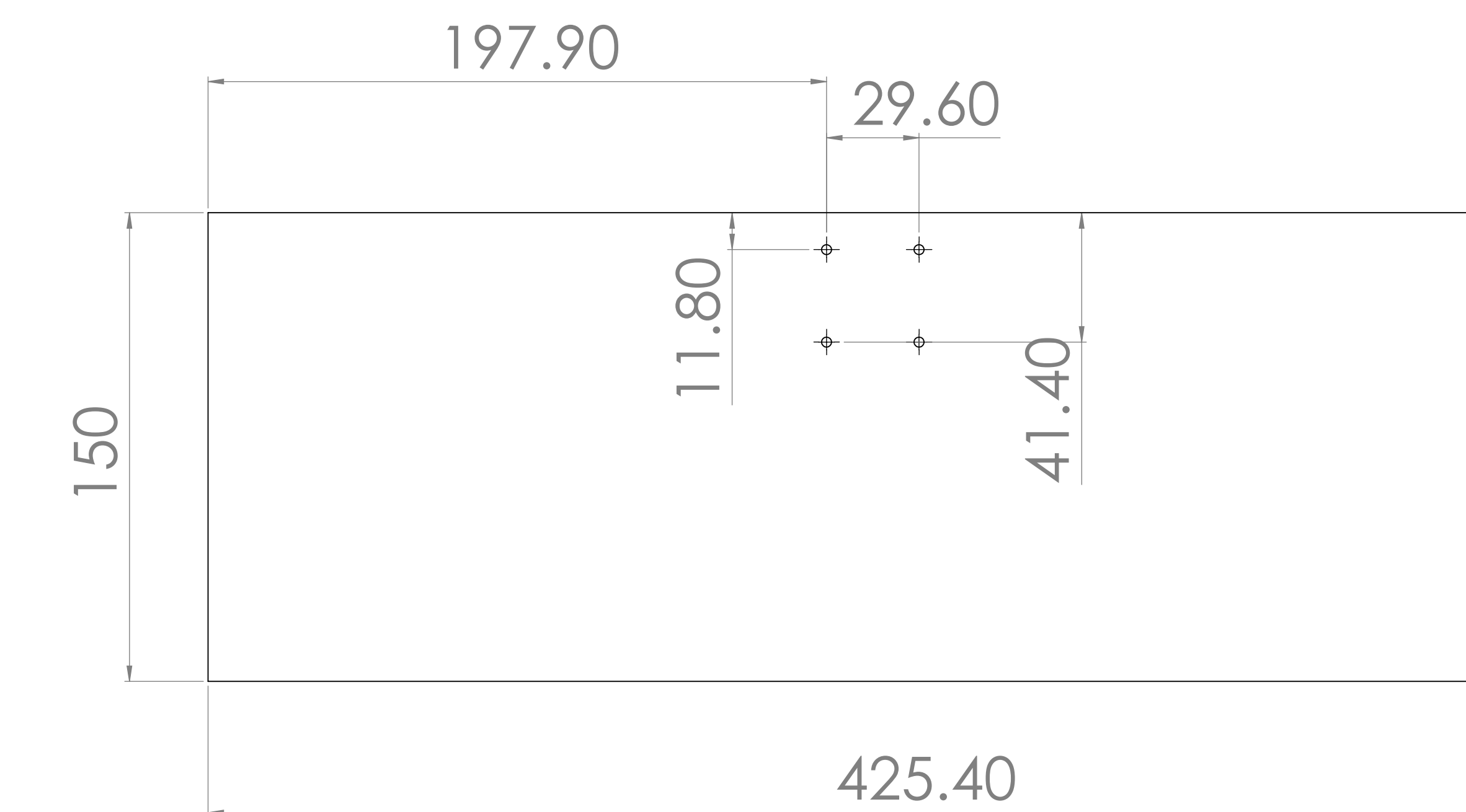




# Pulley Mounting Plate



# Linear Actuator Mounting Plate

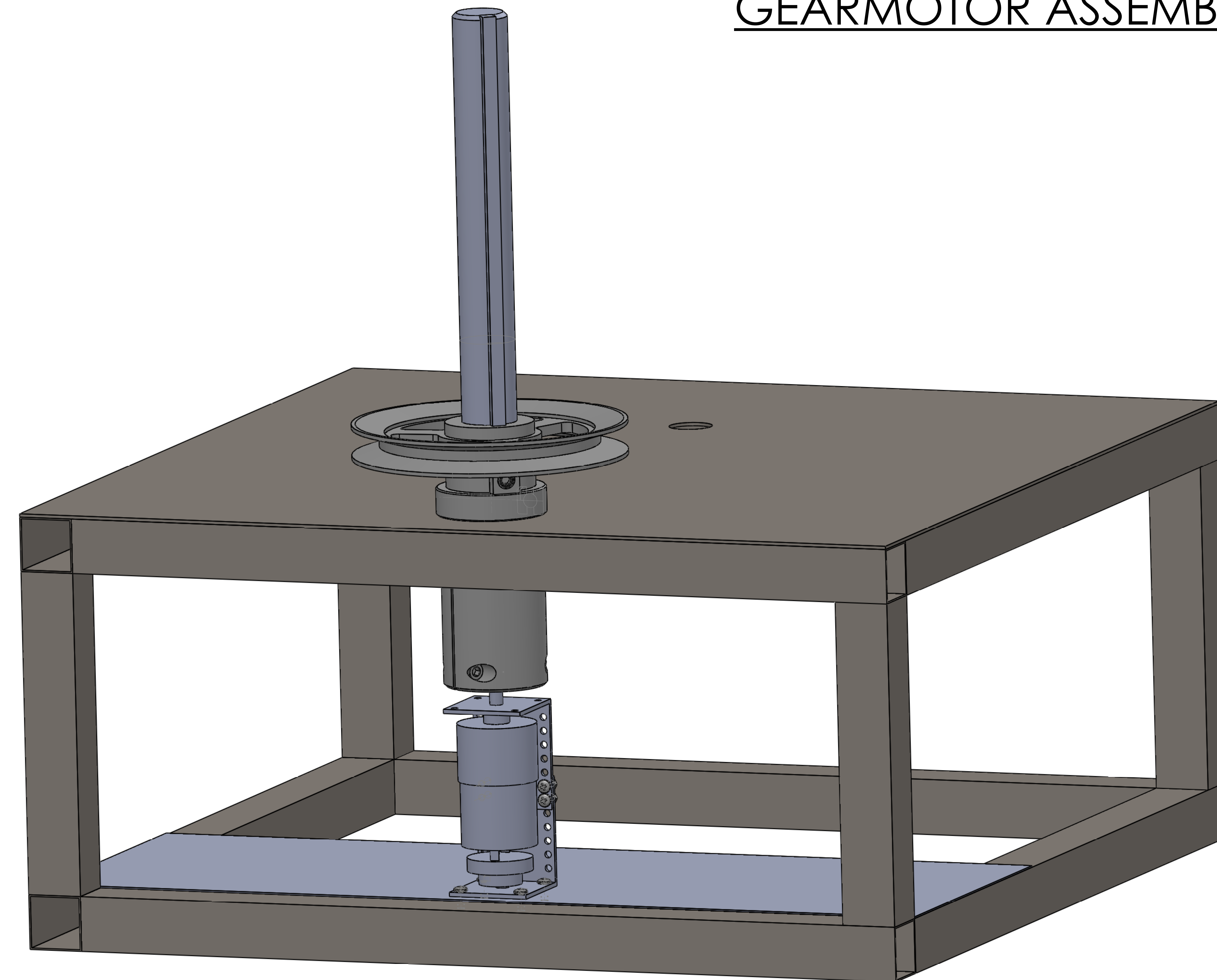


# Gearmotor Mounting Plate

A horizontal line graph representing a constant value. The y-axis is labeled "0.76". A single horizontal line extends from the y-axis at approximately 0.76 to the right, indicating a constant function.

# General Thinkness for all plate.

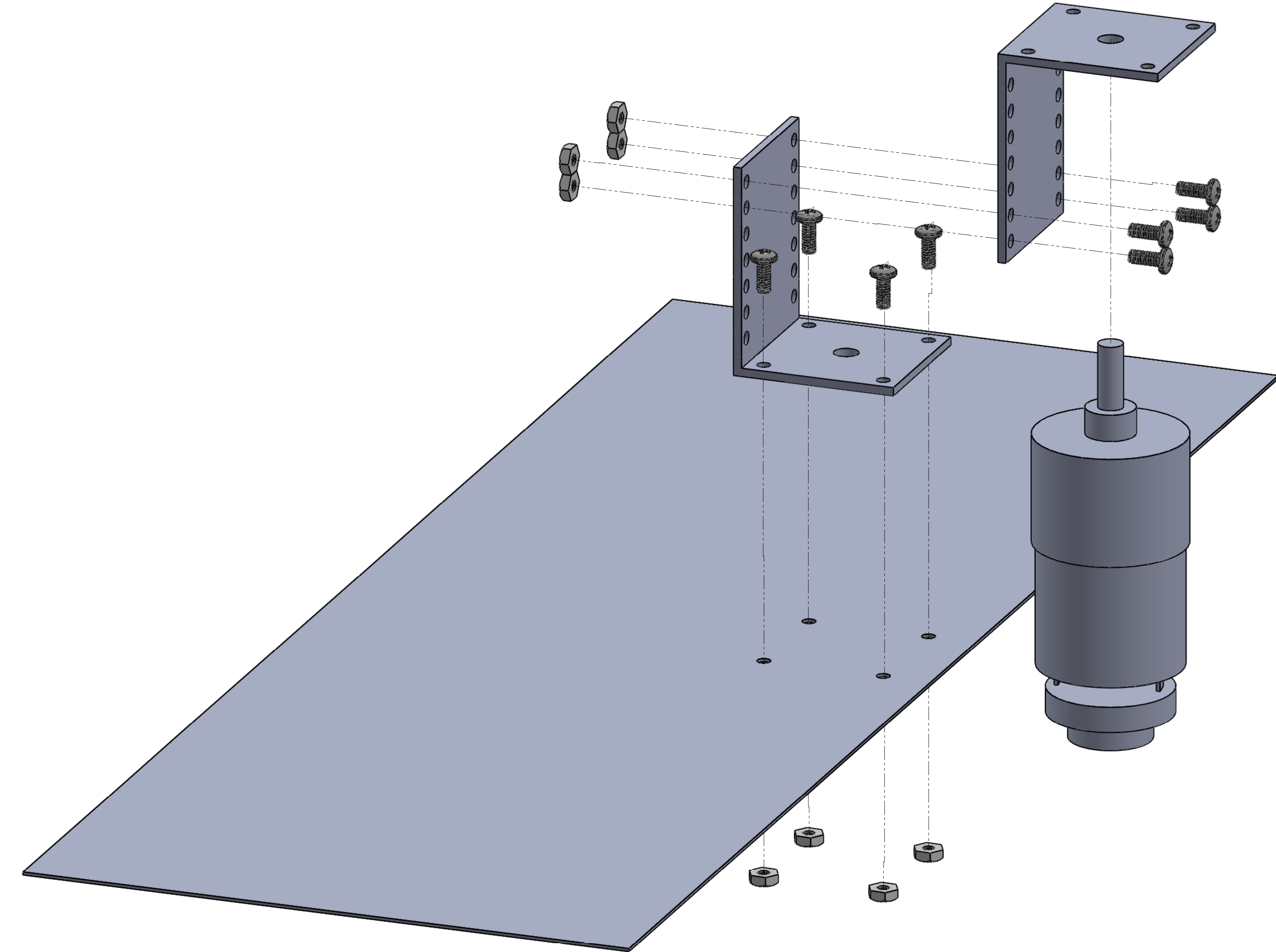
# GEARMOTOR ASSEMBLY



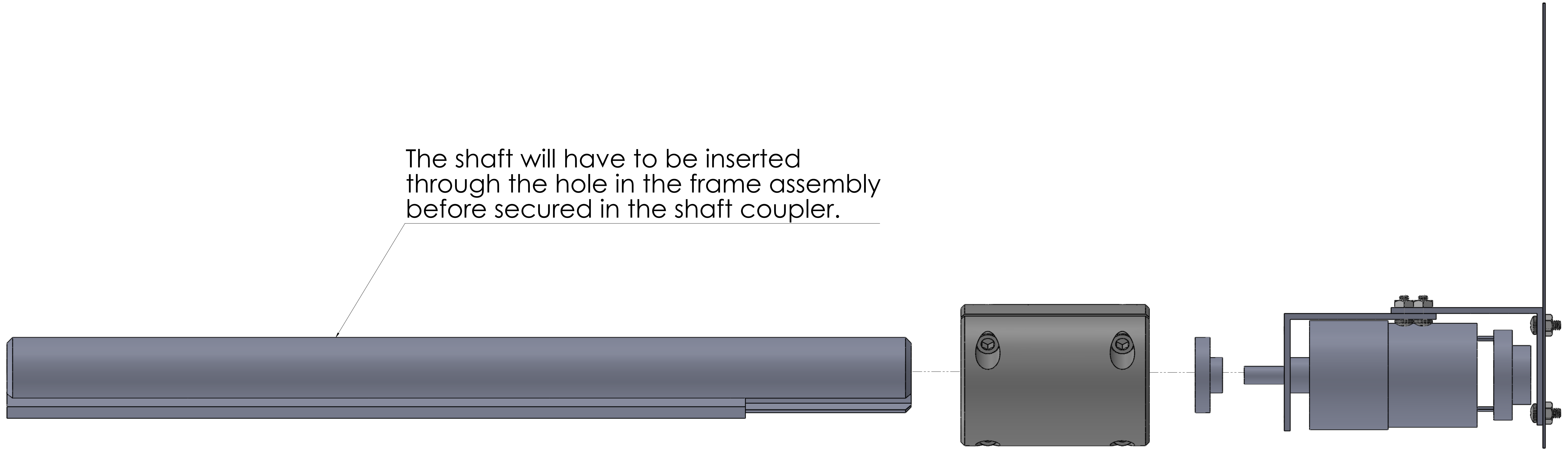
**SolidWorks Student Edition.  
For Academic Use Only.**

UNLESS OTHERWISE SPECIFIED: ALL DIMENSIONS ARE IN MILLIMETERS	FINISH:	DEBUR AND DEBUSH SHARP EDGES	DO NOT SCALE DRAWING	REVISION
DRWNS:	NAME:	SIGNATURE:	DATE:	101:
CKD:				
CAP:				
MFG:				
G.A.				
MATERIAL:				
WEIGHT:				

DWG NO.: Gearmotor Assembly A1  
SCALE: 1:2 SHEET 1 OF 4

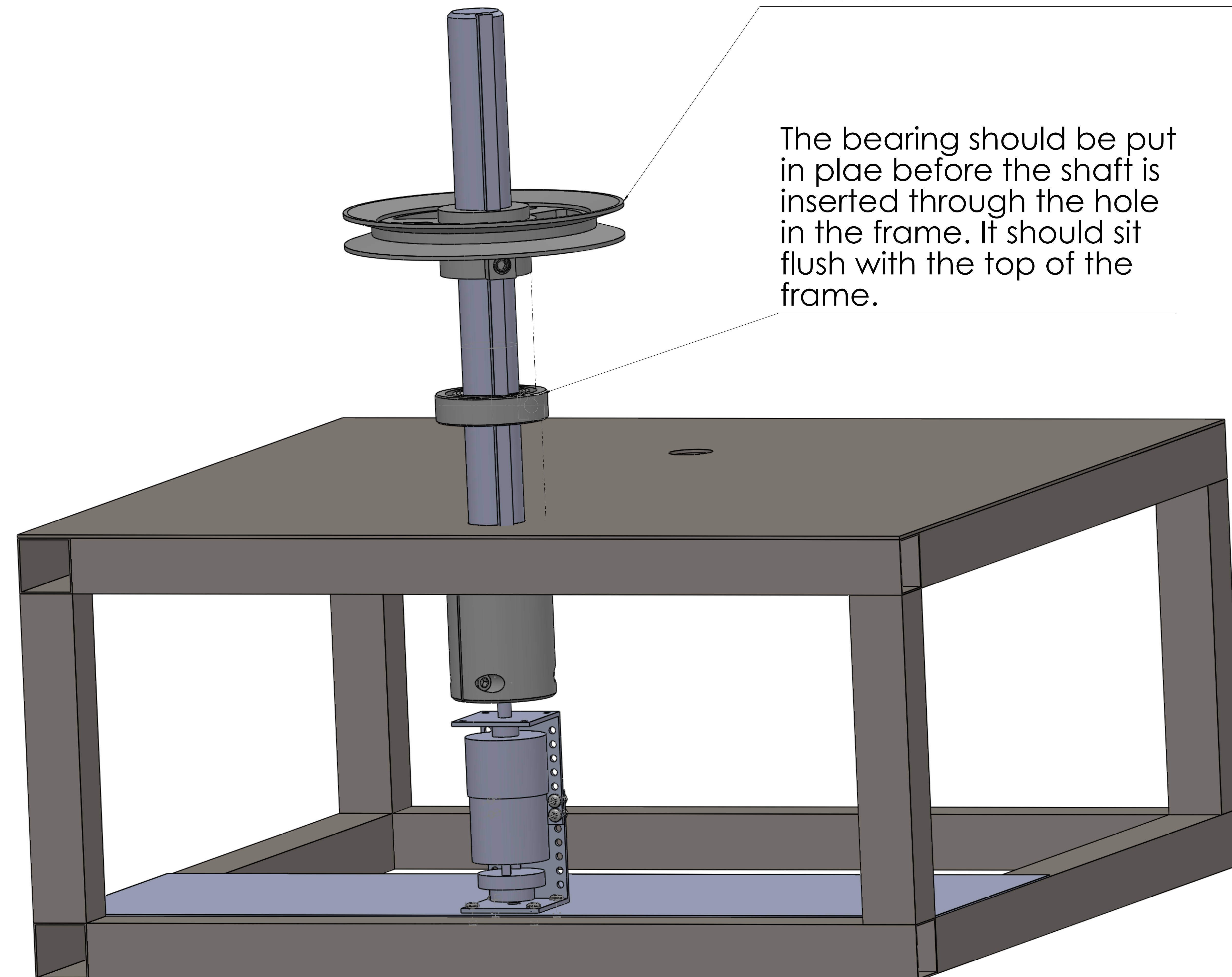


First the gearmotor must be attached to the top L-Bracket. Then the two L-Brackets can be connected. Once it is assembled it can be fastened to the bottom plate that is attached to the frame.



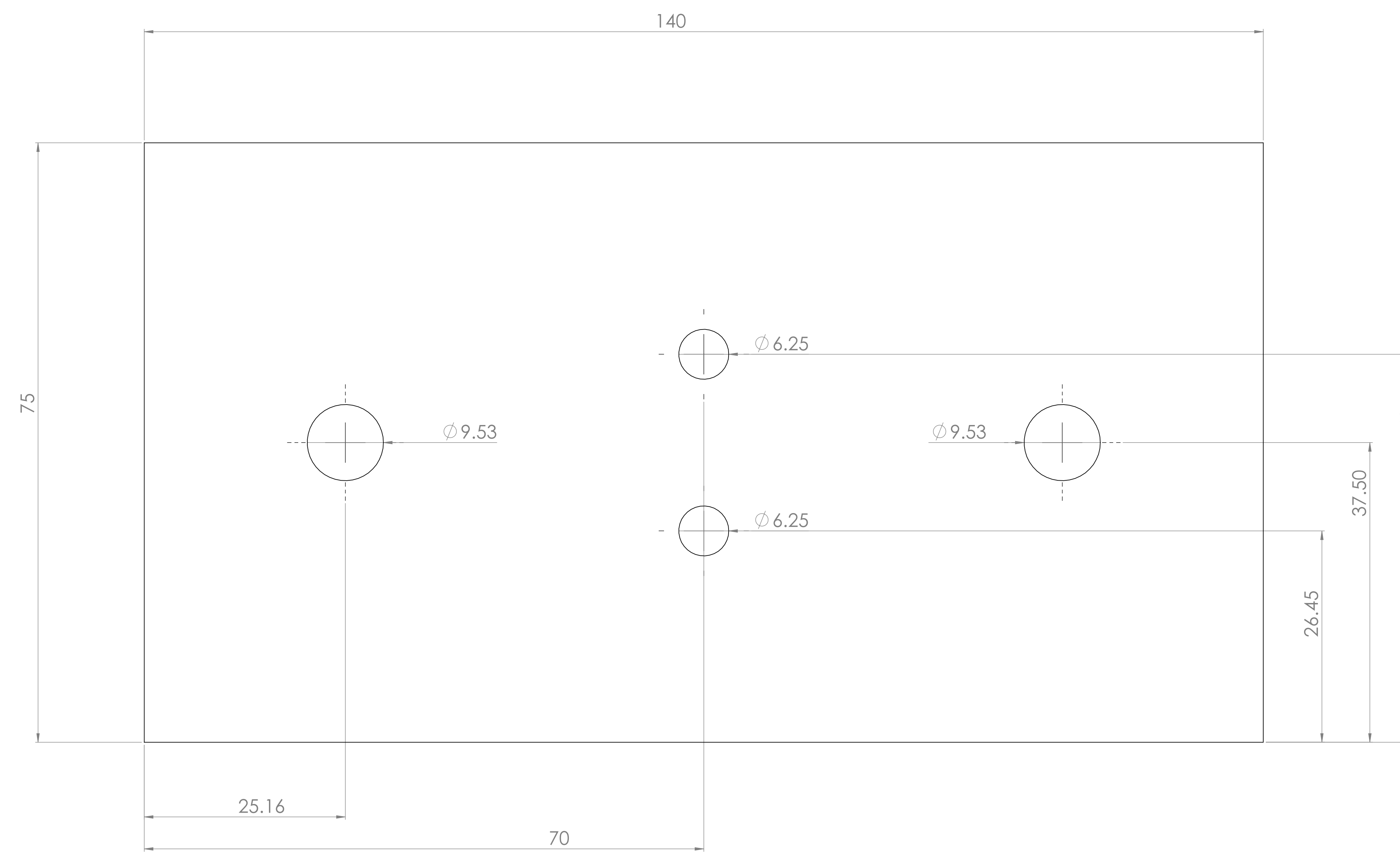
The shaft will have to be inserted through the hole in the frame assembly before secured in the shaft coupler.

The next step is to attach the 6mm mounting hub to the motor with the set screw. Next place the 1" shaft coupler over the hub while also inserting the keyed shaft through the opposite end. Tighten the shaft coupler to secure the shaft and motor together.

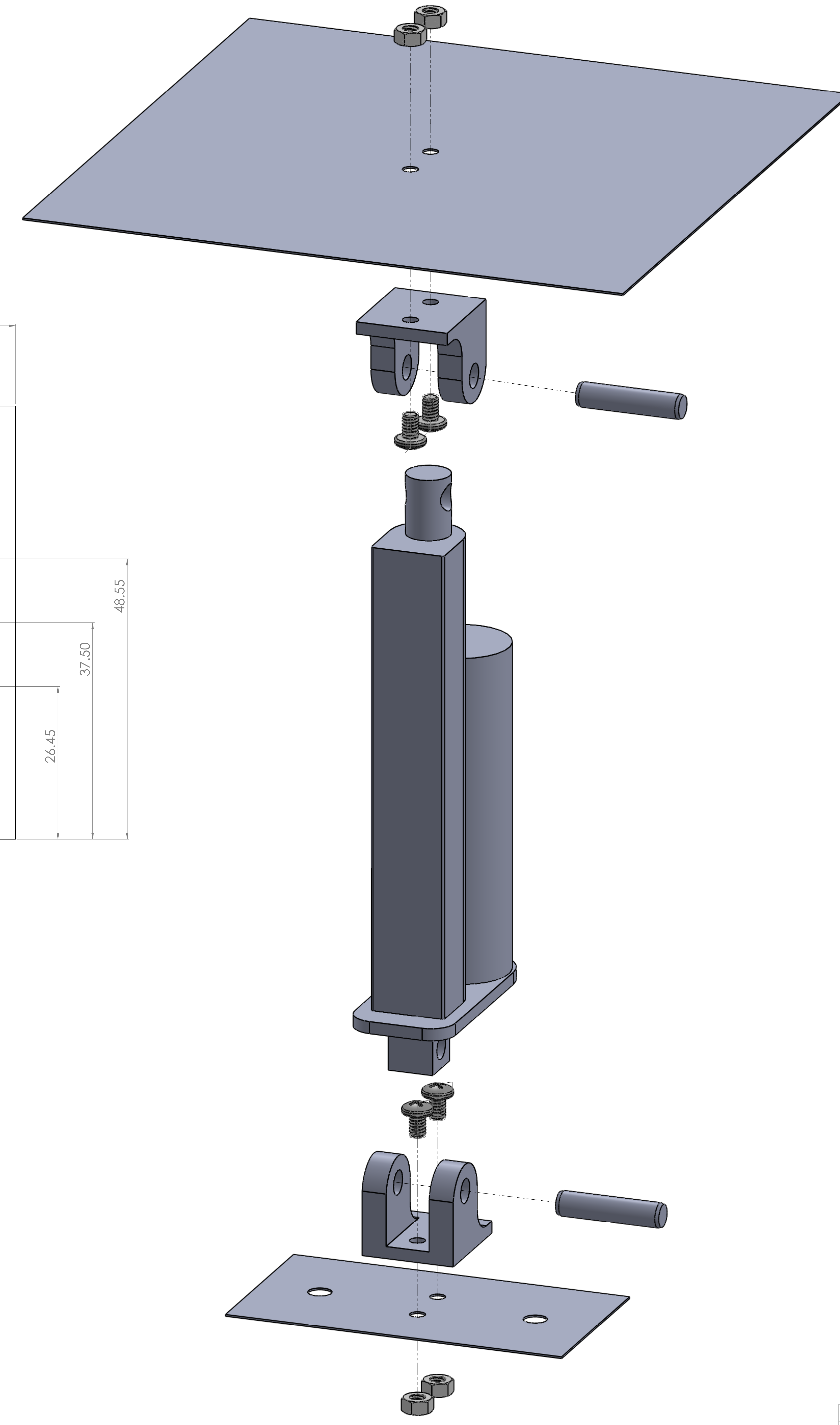


The V-Belt pulley can be placed on the shaft last and secured with the set screw.

The bearing should be put in place before the shaft is inserted through the hole in the frame. It should sit flush with the top of the frame.



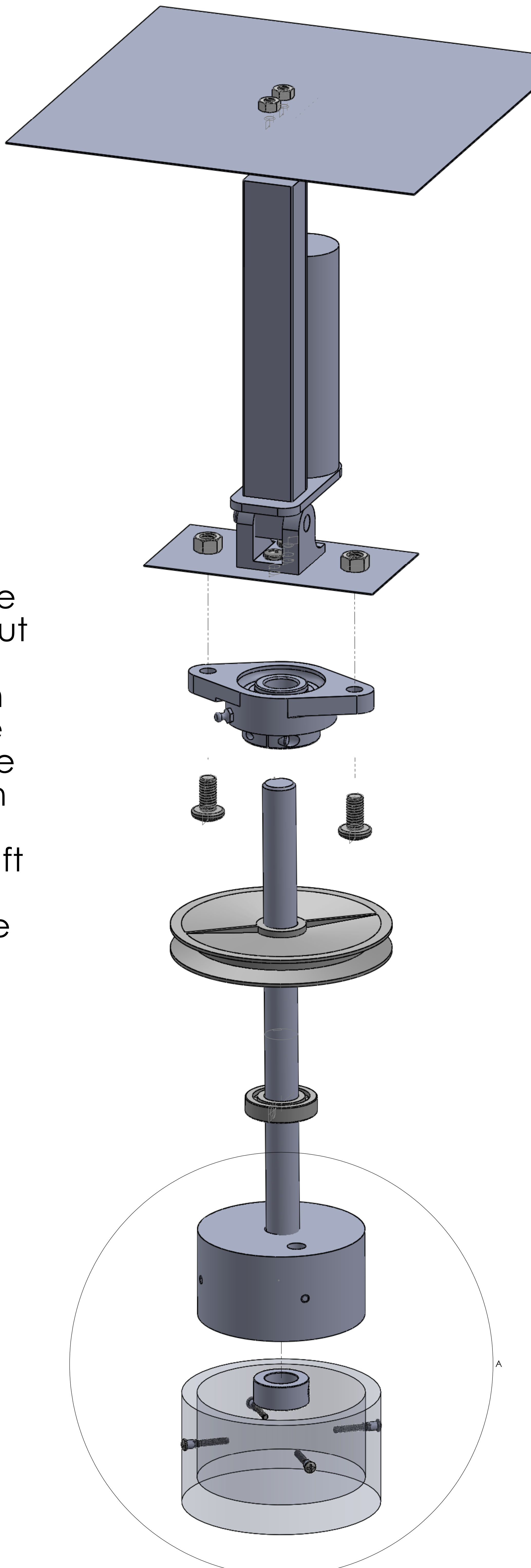
Mounted Concentric Bearing Mounting Plate



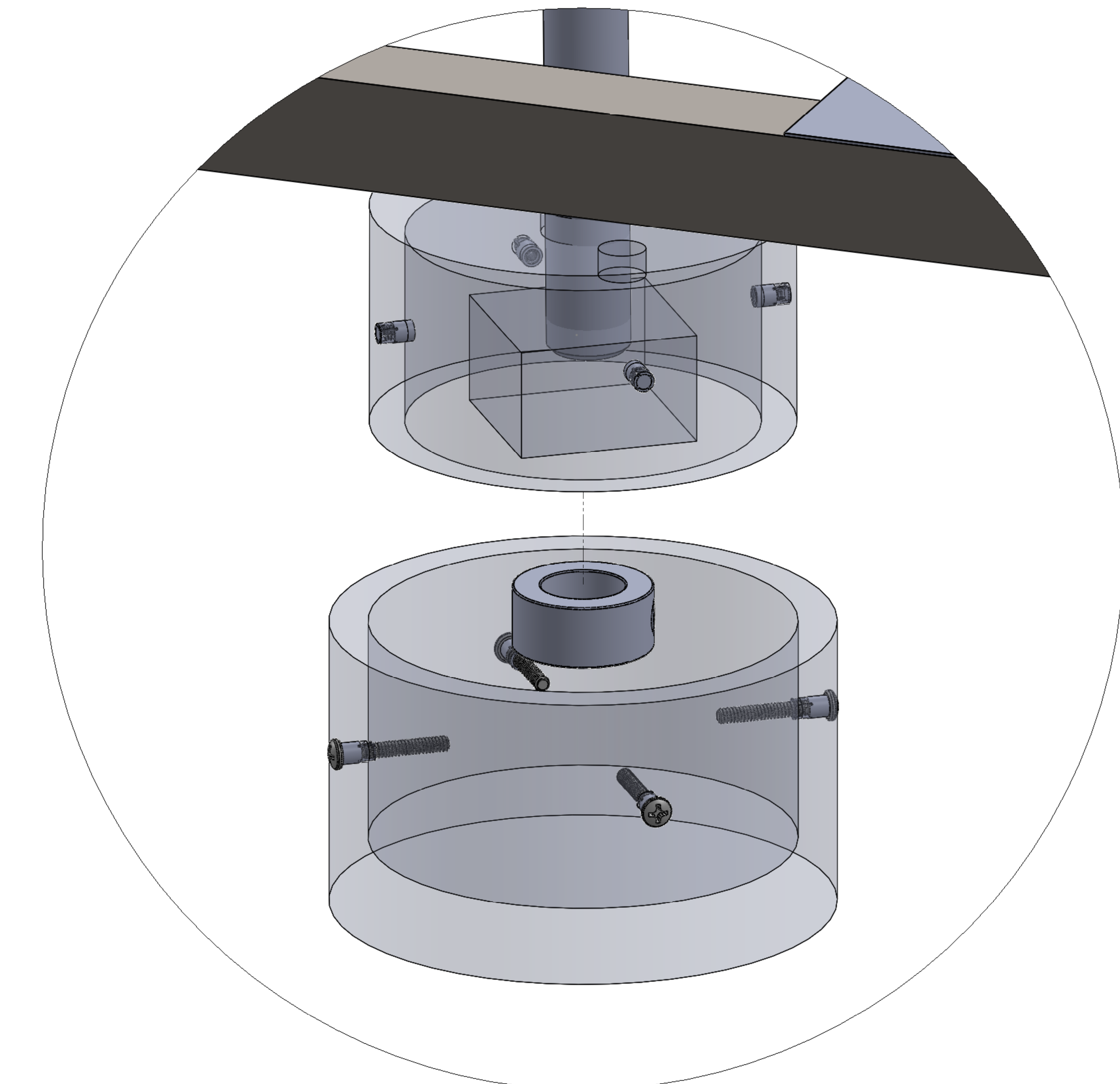
UNLESS OTHERWISE SPECIFIED:	FINISH:	DEBUR AND BROACH SHARP EDGES	DO NOT SCALE DRAWING	REVISION
ALL DIMENSIONS ARE IN MILLIMETERS				
SURFACE FINISH:				
DEBUR:				
LINEAR:				
ANGULAR:				
DRAWN:	NAME:	SIGNATURE:	DATE:	
CHKD:				
CORR:				
MFG:				
G.A.				
	MATERIAL:			
	DRAWN BY:			
	DATE:			
	SCALE:			
	WEIGHT:			

Linear Actuator assembly

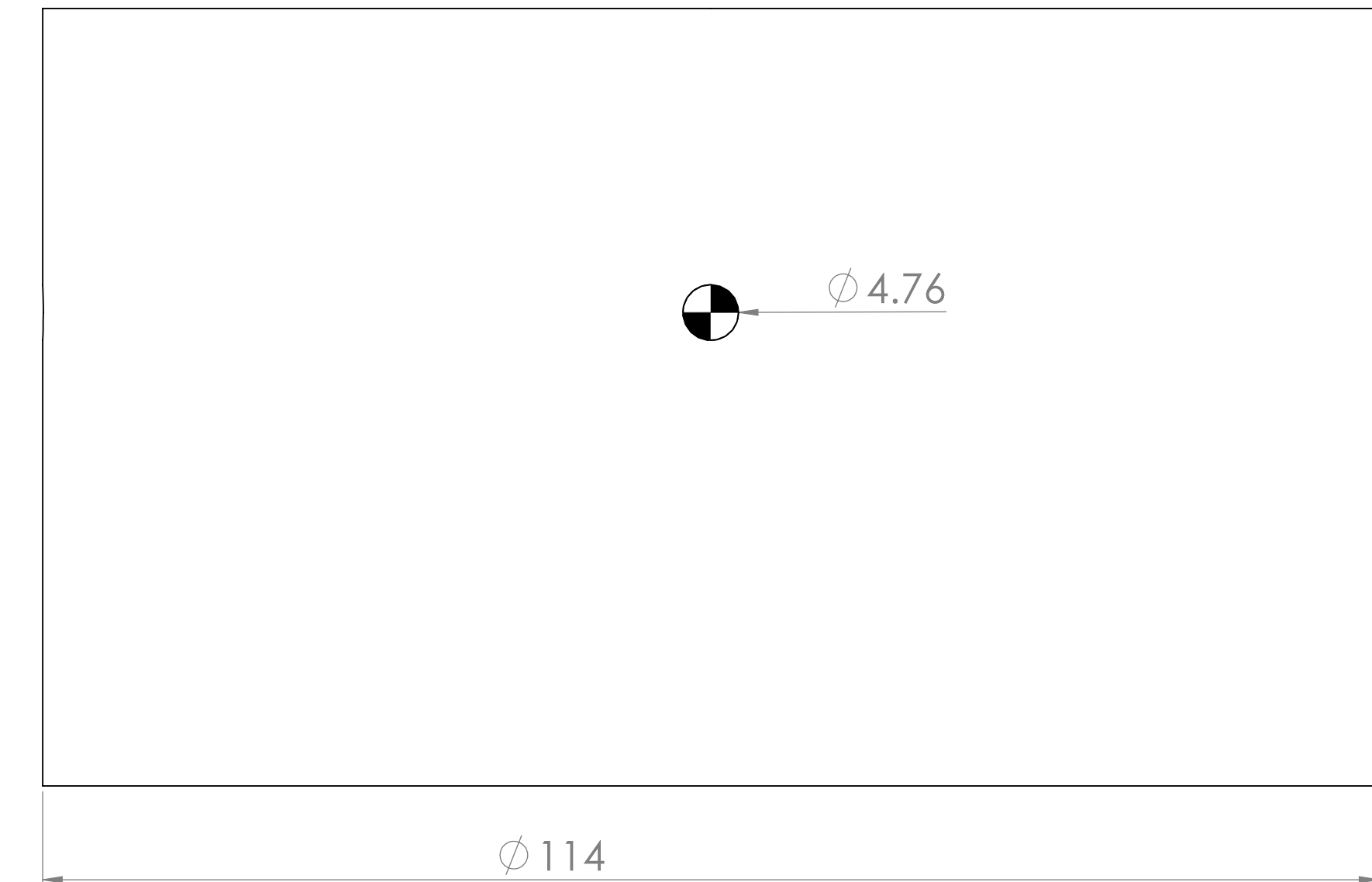
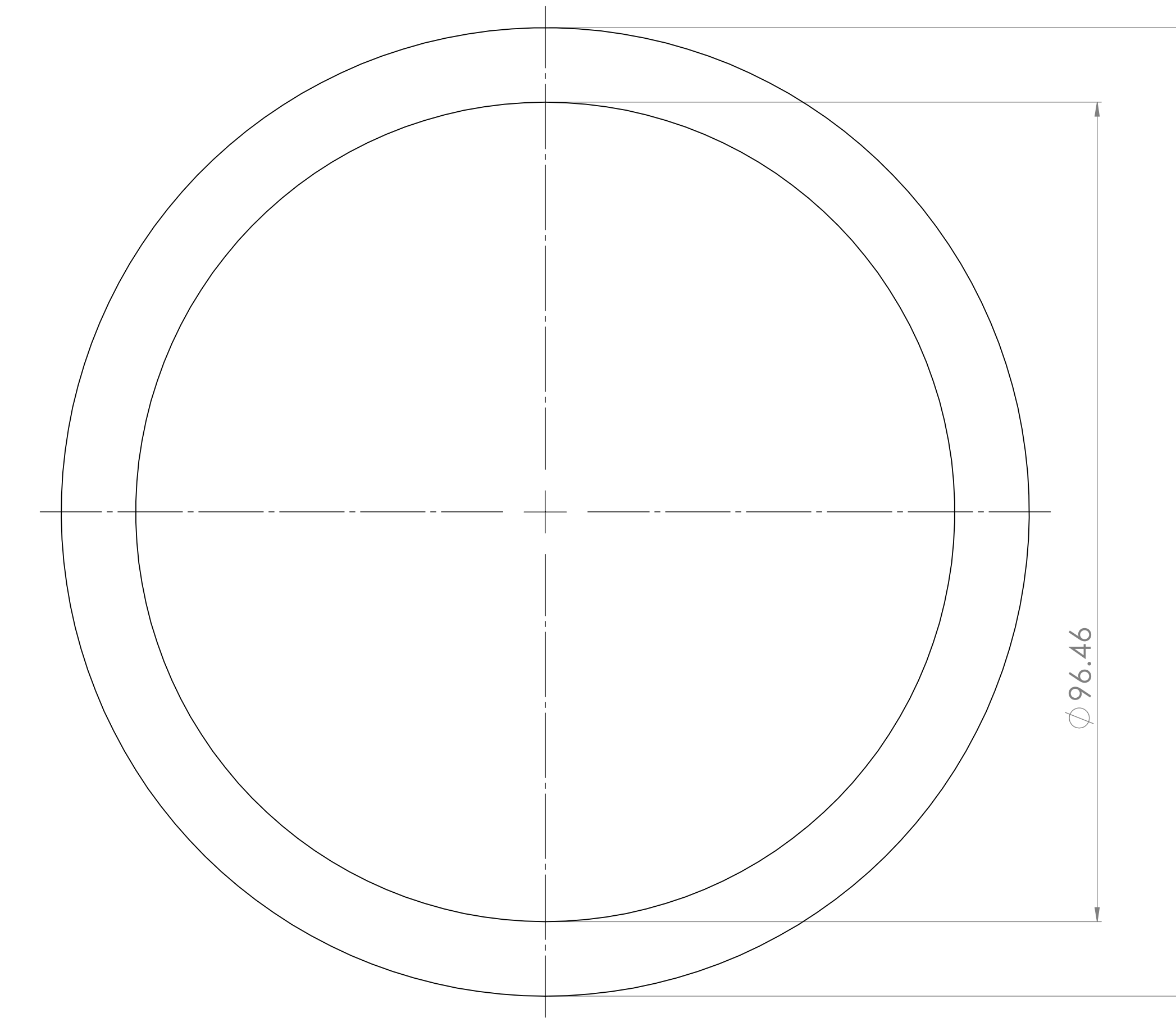
At this part of the assembly the pulley and bearing must be put in position on the pulley mounting plate. The shaft can then be fed through the plate and two components from the bottom of the frame and then secured in the mounted bearing. Lastly there is the shaft collar which is to be installed after the top of the base plate is mounted to the shaft.



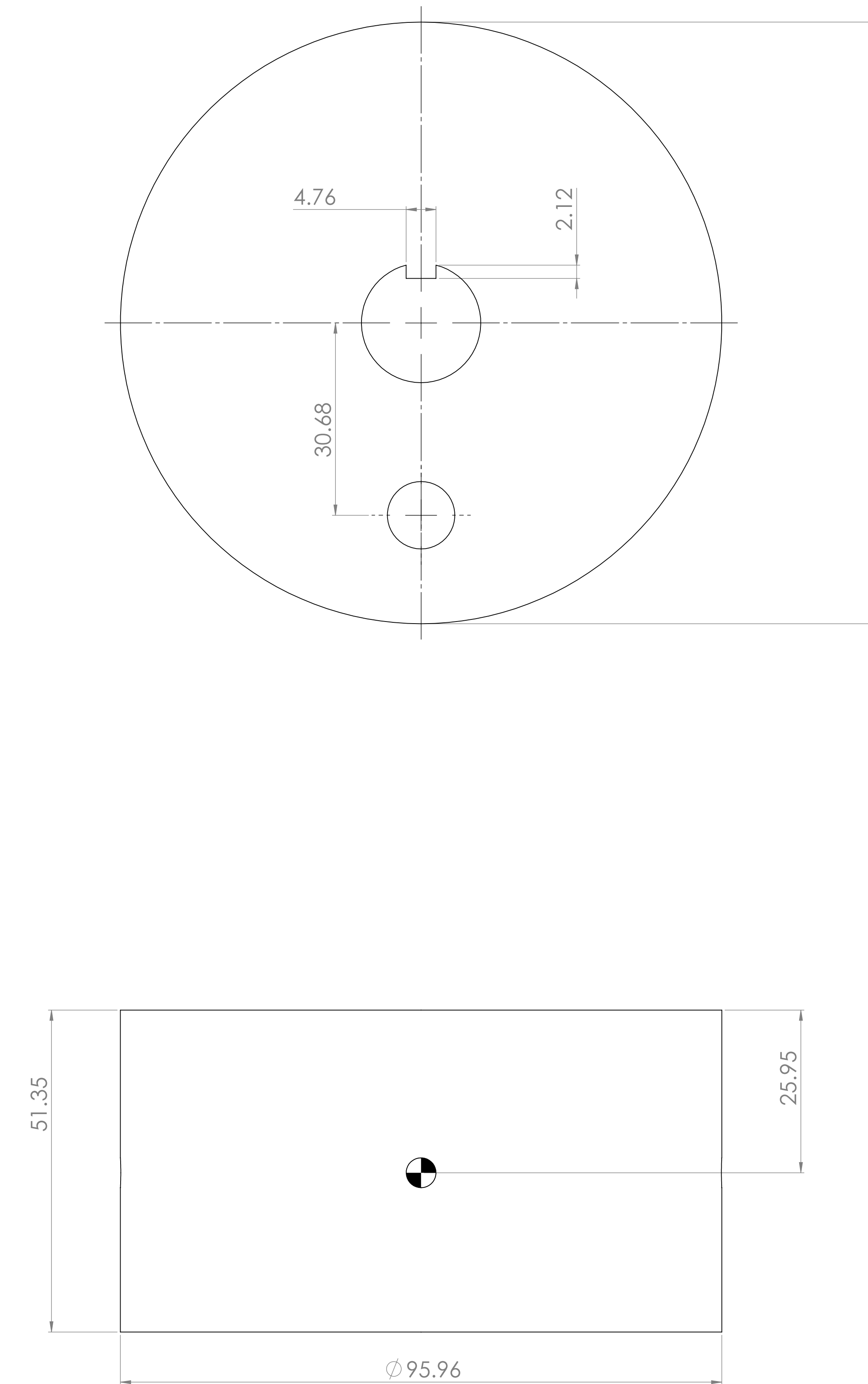
DETAIL A  
SCALE 18 : 10



The top of the base plate must be placed on the shaft prior to the shaft collar being secured. The bottom of the base plate can then be positioned and secured to the top with the four screws.



# BASE PLATE BOTTOM



BASE PLATE TOP